JOC The Journal of Organic Chemistry

Article

pubs.acs.org/joc

Electronic, Spectroscopic, and Ion-Sensing Properties of a Dehydro[*m*]pyrido[14]- and [15]annulene Isomer Library

Paul N. W. Baxter,*[,†] Abdelaziz Al Ouahabi,[†] Jean-Paul Gisselbrecht,[‡] Lydia Brelot,[∥] and Alexandre Varnek[§]

[†]Institut Charles Sadron, UPR 22-CNRS, 23 rue du Loess, Strasbourg, France

[‡]Laboratoire d'Electrochimie et de Chimie Physique du Corps Solide and [§]Laboratoire d'Infochimie, Université de Strasbourg, UMR 7177-CNRS, 4 rue Blaise Pascal, Strasbourg, France

[∥]Service de Radiocristallographie, Université de Strasbourg, UMR 7177-CNRS, 1 rue Blaise Pascal, Strasbourg, France

Supporting Information

ABSTRACT: An isomeric series of dehydro[*m*]pyrido[*n*]-annulenes incorporating strained 1,4-buta-1,3-diyne units have been synthesized, where $m = 2$, $n = 14$ (**1a**–**d**); $m = 2$, $n = 15$ (**2a**,**b**); and $m = 3$, $n = 15$ (**3**). The number of pyridine rings and annulene ring π-electrons are denoted by m and n, respectively. The X-ray crystal structures of **1b** and **1c** confirmed their cyclic formulation. All macrocycles were found to be luminescent chromophores with differing isomer-dependent proton and metal ion-sensory emission responses, which appear collectively as analyte-specific color patterns. Within the series studied, **1a** was singular in displaying the highest luminescence quantum yield and sharing the strongest emission energy and molar absorption changes upon protonation and Hg^{II} binding. Spectroscopic and electrochemical results were supported by density functional theory calculations in showing **1a**, **2a**, and **3** to be low bandgap materials with lowest unoccupied molecular orbitals delocalized over the 1,4-di(pyridin-4-yl)buta-1,3-diyne bridges that provide a pathway for electronic communication between the nitrogens. Overall, the investigations suggest that **1a**, **2a**, and **3** would be excellent ligands for the construction of novel conjugated hybrid metallosupramolecular nanostructures, polymers, and ion-sensory systems.

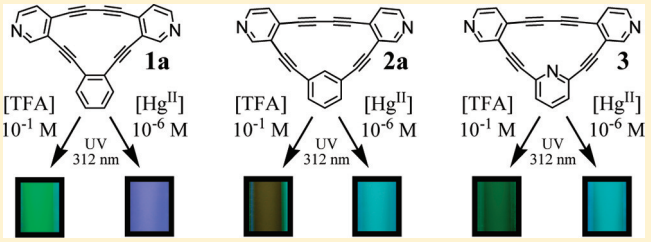

INTRODUCTION

Dehydroaryl[*n*]annulenes[1−7] are a class of cyclically conjugated hydrocarbons that are currently the focus of considerable interest within the physical and chemical community. For example, dehydrotribenzo[12]- and [18]annulenes represent the elementary structural units of graphyne and graphdiyne, respectively, which are hypothetical expanded carbon networks predicted to possess many intriguing mechanical and physicochemical properties.[8−15] Further structural elaboration of these dehydrobenzo[*n*]annulenes may in the future yield sections or fragmental model systems of such polymers.[16−22] Specific dehydrobenzo[*n*]annulenes have recently been shown to act as NLO chromophores with potential two-photon absorption properties[23−25] and to function as new types of photochromic,[26,27] high spin magnetic,[28−30] and liquid crystalline materials,[31,32] as well as electronic conductors when doped.[33] They are also high-energy storage substrates, particular examples serving as precursors for the generation of carbon buckyonions and nanotubes,[34−37] as well as constituting interesting novel strained-ring systems.[38−47] Within the field of supramolecular chemistry, they have been reported to function as assembly units for the generation of pseudorotaxane type architectures[48] and to form well ordered two-dimensional crystalline layers on specific interfaces.[49] They may also undergo intramolecular rearrangements to give novel polyaromatic hydrocarbons[47,50,51] and continue to serve as targets for theoretical modeling, to gain further insight into their aromaticity and spectroscopic and electronic properties.[41,52−60]

We have been particularly interested in exploring the physicochemical properties of the dehydro[*m*]pyrido[*n*]-annulenes, for example, **4**–**6** (Chart 1),[61] which are nitrogen-heterocyclic analogues of the dehydrobenzo[*n*]annulenes that are capable of binding metal ions directly to the heteroatoms situated on the outer surface of the macrocyclic ring.[62−68] Some of these and related macrocycles were discovered to function as luminescence ion sensors[61,69,70] and to afford coordination network polymers with specific metal salts.[71] Coordination polymers incorporating dehydro[*m*]pyrido[*n*]annulene repeat units, which topologically mimic theoretically proposed all-carbon networks, are attractive synthetic targets because they may be expected to display a rich variety of exploitable properties such as electrochemical, photochemical, magnetic, optical, catalytic, porous, inclusion, sensory, and mechanical behavior.[72−74]

Received: July 31, 2011
Published: December 1, 2011

Chart 1

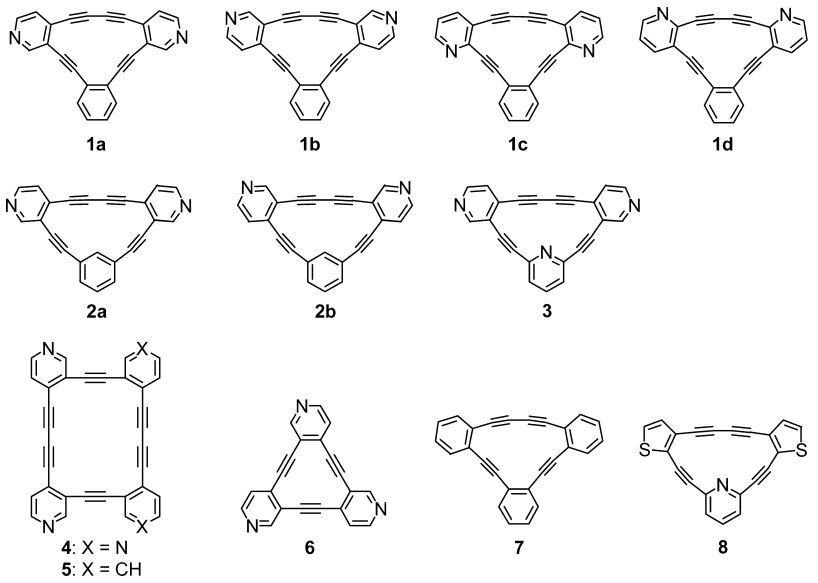

In particular, the incorporation of metal ion-binding pyrido-analogues of the internally strained dehydrotribenzo[14]-annulenes of type **7**[46] and its [15]annulene isomer[44] into coordination polymers and oligomers may yield materials with topologically interesting curved pathways for intermetal electronic communication. The ligands themselves may also exhibit characteristic spectroscopic perturbations upon metal ion-binding with potential ion-sensing applications.

With these considerations in mind, however, we first needed to determine which of the many possible isomers within the dehydro[*m*]pyrido[14]- and [15]annulene series would be optimally suited for the creation of coordination polymers and ion sensors.

We therefore present below an investigation into the comparative spectroscopic and ion-binding properties of an isomer library of dehydro[*m*]pyrido[14]- and [15]annulenes **1a**–**d**, **2a**,**b**, and **3**, supported by electrochemical and density functional theory (DFT) investigations. These studies predict that **1a**, **2a**, and **3** would be best suited for the assembly of electronically conjugated coordination polymers and oligomers and suggest that ion-sensory applications would be most efficiently achieved collectively, involving libraries of macrocycles rather than with specific isomers. It may be noted that the spectroscopic properties of some structurally related dehydro[*m*]pyrido[*n*]annulenes such as, for example, **8**, have been reported[75−77] but differ electronically in being donor–acceptor systems with nitrogens more sterically constrained for metal coordination and for which no metal ion-binding studies have been reported.

■ RESULTS AND DISCUSSION

The syntheses of **1a**–**d**, **2a**,**b**, and **3** were achieved using standard Sonogashira and Eglinton–Galbraith coupling methodology, from a series of regiochemically defined monoprotected *ortho*-diethynylpyridine isomers, the details of which are described in the Supporting Information. The structural formulation of all products was established on the basis of mass spectroscopic, infrared, ^{1}H and ^{13}C NMR spectroscopic studies, and, when necessary, correlation spectroscopy, heteronuclear multiple quantum coherence (HMQC), and/or heteronuclear single quantum coherence (HSQC) measurements and spectral comparisons with their respective precursors. It may be noted that despite the fact that cycles **1a**–**d**, **2a**,**b**, and **3** were strained molecules, they were found to be indefinitely stable in the solid state at ambient temperature as well as in CH_2Cl_2 solution over several months, in the absence of light. Although stable to silica gel, they were found to be best purified by chromatography on neutral or basic alumina, as is often the case with polypyridine ligands, due to their enhanced basicity.

Solution Aggregation of 1a. As planar aromatic macrocycles are frequently known to form aggregates in solution,[61,78−80] we investigated the possibility of aggregation effects in the case of **1a**, as it was one of the least soluble macrocycles within the series studied, and formed a fibrous microcrystalline solid upon solvent evaporation suggestive of strong intermolecular association. The ^{1}H NMR spectrum of **1a** in $CDCl_3$ did indeed exhibit upfield displacements in proton chemical shifts upon solution concentration, indicative of aggregation phenomena and supportive of its planar structural formulation (see the Supporting Information for details). However, measurement of the hydrodynamic radius using the diffusion ordered spectroscopy (DOSY) technique[81] afforded a value of 4.3 Å, corresponding to single molecules or weak associations of no more than two molecules of **1a**, suggesting fast association–dissociation on the NMR time scale.

X-ray Crystal Structural Characterization of 1b and 1c. An X-ray crystal structural analysis of suitable crystals of **1b** and **1c** grown from $CDCl_3$ confirmed the macrocyclic identity and strained nature of these systems and revealed that they both possess a small triangular internal cavity (Figure 1, upper left). As expected, **1b** is planar; yet, **1c** is distinctly nonplanar, with the benzene ring positioned to one side of the mean plane through the 1,4-di(pyridin-3-yl)buta-1,3-diyne moiety and pointing away from it (Figure 1, upper right).

In contrast to the hydrocarbon analogue **7**,[46] cycles **1b** and **1c** do not stack into columns with the 1,4-diarylbuta-1,3-diyne units in parallel overlay optimal for topotactic polymerization. Instead, the crystal packing of **1b** and **1c** comprise tilted "head to tail" rows of macrocycles, which rest upon each other in alternate directions and collectively form close-packed sheets (Figure 1, center left and right). The alternate directional

dx.doi.org/10.1021/jo201595s | J. Org. Chem. 2012, 77, 126–142

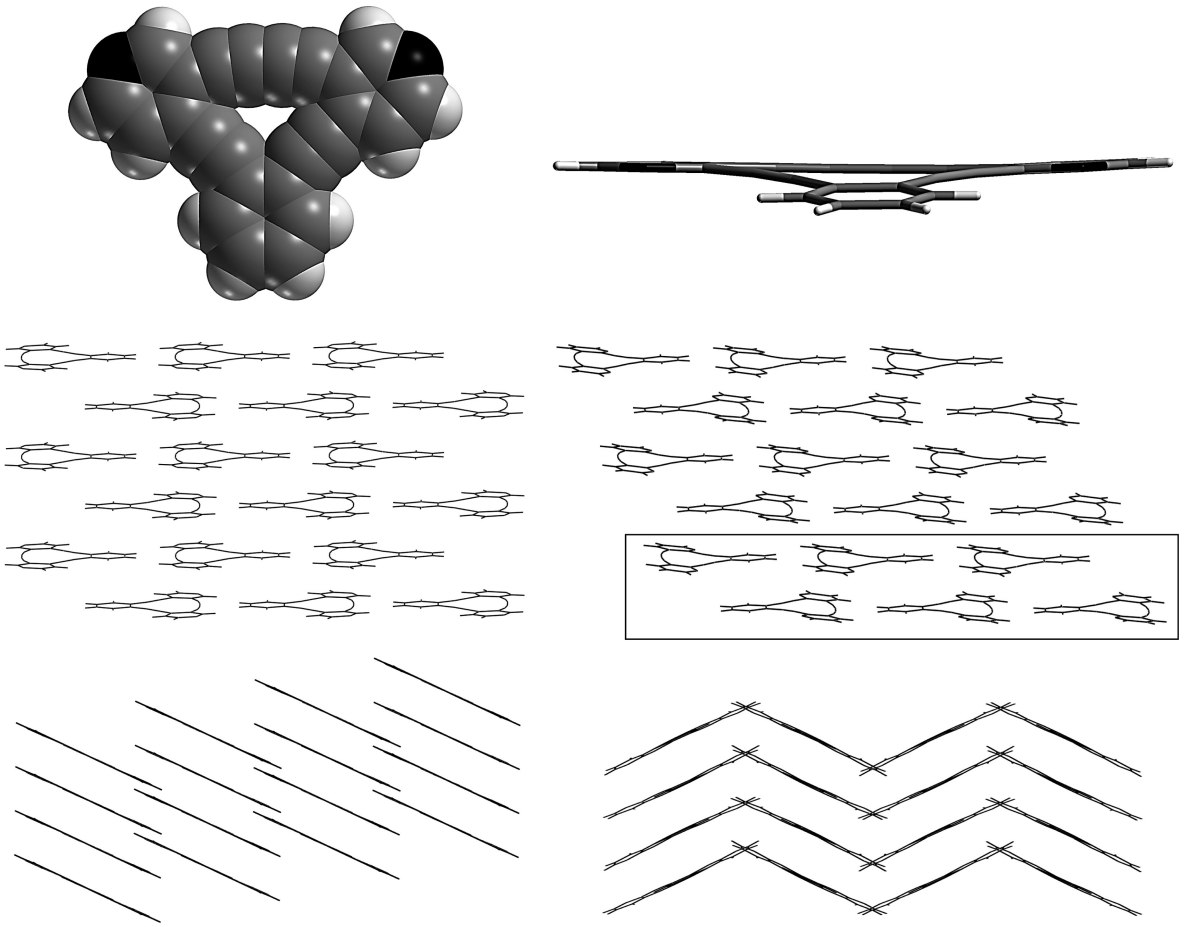

Figure 1. X-ray crystal structures of **1b** and **1c**. Plan view of **1b** (space-filling representation), upper left; and stick representation of **1c**, view through the 1,4-di(pyridin-3-yl)buta-1,3-diyne mean plane, upper right (the benzene is in the foreground). View of the b−c plane (sheet) of **1b** showing alternate antiparallel rows of macrocycles (center left), and view along the *b*-axis showing the arrangement of tilted sheets of **1b** (lower left). View of the a−c plane (sheet) of **1c** showing alternate antiparallel rows of macrocycles (center right), and view through the *c*-axis showing zigzag arrangement of tilted sheets of **1c** (lower right). In the center right view, the lowest pair of overlaid rows of **1c** is highlighted by enclosure within a rectangle.

packing between the rows of **1b** and **1c** ensures that the pyridine ring dipoles avoid parallel alignments, thereby minimizing intermolecular repulsions. However, the arrangement of the rows of **1c** relative to each other differs from **1b** in that the 1,4-di(pyridin-3-yl)buta-1,3-diyne and benzene moieties directly overlay each other only within pairs of rows. Each pair of overlaid rows is displaced from the next pair such that the benzenes of one pair lie over the faces of the macrocycles of the adjoining pair (Figure 1, center right). Indeed, this packing arrangement appears responsible for the nonplanarity of **1c**, as the benzene rings are bent into the faces of the overlying macrocycles at the interface between each adjoining pair of rows.

In **1b** and **1c**, the shortest interpyridine contacts are, respectively, 3.380 and 3.324 Å, and in **1c**, the shortest interbenzene contact is 3.372 Å, all of which are within the Van der Waals radii. Aromatic $\pi-\pi$ stacking interactions and dipole alignments therefore significantly control the packing motifs in the latter two macrocycles.

Cyclic Voltammetric Studies. In view of the electrochemical activity reported for dehydroaryl[*n*]annulenes and related systems,[33,82−84] we anticipated that our dehydro[*m*]-pyrido[14]- and [15]annulenes may also be electrochemically active, especially toward reduction, a property that would be of importance for electron transport within hybrid conjugated metallopolymers incorporating these ligands. To explore this possibility, we performed electrochemical investigations on **1a**, **2a**, and **3**, the systems anticipated to have the most effective pathways for internitrogen electronic communication, as well as acyclic **9**[61] for comparison.

In the case of the dehydro[*m*]pyrido[15]annulenes **2a** and **3**, at relatively low scan rates (0.1 V s^{-1}), one well-resolved reversible one-electron reduction step is observed at −1.71 and −1.70 V *vs* Fc^+/Fc as well as a second irreversible reduction at *E*pc = −2.05 and −2.03 V *vs* Fc^+/Fc, respectively. This second reduction became reversible at scan rates higher than 1 (**2a**) and 2 V s^{-1} (**3**), with the corresponding redox potentials being observed at −1.73 and −1.98 V for **2a** and −1.69 and −1.93 V for **3** *vs* Fc^+/Fc, respectively (Table 1 and Figure 2), denoting the chemical instability of the generated dianion.

Qualitatively, cycle **3** would be expected to be more easily reduced than **2a** due to the presence of the three comparatively electron-withdrawing pyridine rings in the former. However, the first reversible one-electron reduction and the second irreversible reduction at 0.1 V s^{-1} of **2a** and **3** are very similar, within the accuracy of potential determination, revealing that the presence of the central pyridine nitrogen in **3** has a negligible effect upon the reduction potentials. Within the dehydro[*m*]pyrido[15]annulene series, the lowest unoccupied molecular orbitals (LUMOs) involved in the reductions

dx.doi.org/10.1021/jo201595s | *J. Org. Chem.* 2012, 77, 126−142

Table 1. Electrochemical Data of 1a, 2a, 3, and Precursor 9 Observed by Cyclic Voltammetry (CV) in CH_2Cl_2 with 0.1 mol/L $[(n\text{-}Bu_4)N]PF_6$[a]

annulene/ precursor	scan rate ($V\ s^{-1}$)[b]	E° ($V_{/Fc+/Fc}$)[c]	ΔEp (mV)[d]	Epc (V)[e]
1a	0.1			−1.78
				−2.14
	5	−1.74	80	
				−2.19
2a	0.1	−1.71	80	
				−2.05
	5	−1.73	110	
		−1.98	130	
3	0.1	−1.70	70	
				−2.03
	5	−1.69	80	
		−1.93	85	
9	0.1			−2.04

[a]All potentials are given *vs* ferrocene, used as internal standard. [b]The CVs at 5 V s^{-1} scan rate were corrected for Ohmic drop before determination of the redox potential. [c]$E^\circ = (Epa + Epc)/2$ where *E*pa and *E*pc are the respective anodic and cathodic peak potentials. [d]ΔEp is the potential difference between the cathodic and the anodic peak potentials. [e]Irreversible peak potential.

therefore appear not to involve the central aromatic ring. This conclusion is further supported by theoretical calculations that show the LUMOs to be mainly nodal on the 1,3-bridging aryl rings of **2a** and **3** (see later).

In contrast, **1a** gave two irreversible reduction peaks at, respectively, *E*pc = −1.78 and −2.14 V *vs* Fc^+/Fc at low scan rates. By increasing the scan rates up to 10 V s^{-1}, only the first reduction became reversible for scan rates higher than 2 V s^{-1}, with a redox potential of −1.74 V *vs* Fc^+/Fc (Table 1 and Figure 2). Reduction of **1a**, an aromatic 14-π electron cycle, would yield a less stable nonaromatic radical, which may therefore undergo a follow-up chemical reaction.

Acyclic **9**, on the other hand, afforded only an irreversible reduction peak at *E*pc = −2.04 V at a scan rate of 0.1 V s^{-1}, identical to those observed for **2a** and **3** (*E*pc = −2.05 and −2.03 V, respectively) at the same scan rate. Increasing the scan rate did not result in reversible behavior, denoting the generation of a species of high reactivity despite the presence of the insulating triisopropylsilyl (TIPS) substituents (Figure 2).

Clearly, cyclization results in a relative stabilization of the monoanion radicals generated upon reduction, a finding suggesting that cyclic dehydroaryl[*n*]annulene type ligands may be superior candidates for achieving electrochemical reservoir behavior and intermetal communication within coordination polymers, as compared to the acyclic arylethynylene ligands frequently used in their construction.

The overall stability toward electrochemical reduction is very similar for **1a**, **2a**, and **3** (E° = −1.74, −1.73, and −1.69 V for **1a**, **2a**, and **3**, respectively, at 5 V s^{-1} scan rate; Table 1), although the [14]annulene **1a** is marginally more resistant to reduction than the [15]annulenes **2a** and **3**. This trend is reflected in the calculated LUMOs of **1a**, **2a**, and **3** (Table 3 and Figure 9), which are also of similar energies and delocalization, yet with that of **1a** lying just above and therefore slightly less reducible than those of **2a** and **3**.

UV−Vis Spectroscopic Studies. The UV−vis absorption spectra of **1a−d**, **2a,b**, and **3** were recorded in CH_2Cl_2 solution at several concentrations within the range 2×10^{-6} to 2×10^{-5} mol/L and showed minimal deviation from the Beer and Lambert law, demonstrating that aggregation was negligible in more dilute solution. Overall, the spectra comprise two main groups of absorption envelopes, the first centered around 300 nm with the greatest molar absorption coefficients, averaging at higher energies for the [15]annulenes as compared to the [14]annulenes (Figure 3). The second group of maxima between 320 and 420 nm are of much lower intensity, with pronounced absorption edge tailing in the case of **2a** and **3**.

The optical bandgaps were also determined from the lowest energy absorption edges of the UV−vis spectra both in solution and in the solid state,[85,86] which show a similar overall trend (Table 2). Thus, the solution optical bandgaps decrease in the following order: **1c** > **1d** > **1b** > **2b** > **1a** > **2a** ≅ **3**. For a given N−N isomer, the dehydro[*m*]pyrido[15]annulenes display lower energy optical bandgaps than their [14]annulene congeners, while those possessing the 1,4-di(pyridin-4-yl)-buta-1,3-diyne unit, that is, **1a**, **2a**, and **3** exhibit the lowest energy bandgaps within the series. The solution UV−vis spectra of all of the macrocycles studied also display absorption edges of lower energy than their respective uncyclized precursors[61,69,70] (Figure 11 in the Supporting Information), emphasizing the bandgap energy-lowering effect of cyclization.

Luminescence Spectroscopic Studies. The luminescence properties of **1a−d**, **2a,b**, and **3** were also investigated, the results of which are summarized in Table 2 and the solution and thin film luminescence emission spectra in Figure 4.

The luminescence spectra of the dehydrodipyrido[14]-annulenes **1b−d** exhibit relatively little variation in shape and energy, whereas that of **1a** is uniquely red-shifted in comparison. In the [15]annulene series, the emission spectra of **2a** and **3** are very similar, highlighting the minor effect that the central pyridine nitrogen of **3** exerts upon the π^* excited state energies, whereas the emission of **2b** is significantly blue-shifted in comparison. The regiochemistry of nitrogen substitution appears therefore to influence the energy of the excited states only in particular cases.

In contrast, the emission spectra of thin films are particularly sensitive to the structural characteristics and surrounding environment of the ligands, showing a continual variation in emission color over 114 nm on passing from **1c** to **3**, and with the [15]annulenes emitting at lower energies than the [14]annulenes.

Luminescence quantum yields were also estimated (Table 2) and, with the exception of **1a**, are all relatively low, falling within the range of 0.02−0.1. Uniquely, cycle **1a** exhibited a quantum yield of 0.26, which is much higher than the overall averaged quantum yield of the other cycles within the series.[87]

Spectroscopic Study of Hg^{II} Binding to 1a−d, 2a,b, and 3. Previous studies revealed that **4−6** and related cycles undergo binding to a range of transition metal ions in dilute solution but in many cases form insoluble precipitates that hamper measurements.[61,69,70] This limitation was not however encountered with Hg^{II}, which also afforded clear and easy-to-follow spectroscopic changes. We therefore decided to evaluate the metal ion-binding properties of **1a−d**, **2a,b**, and **3** using Hg^{II}, with the additional interest that Hg^{II} is an environmental and biological toxin, for which the discovery of new spectroscopic detection methods continues to be in demand.[88−93]

Initially, we probed the binding of Hg^{II} with **1a** over a [**1a**]:[Hg^{II}] range of 1:4−1:100, as this ligand gave the strongest UV−vis response to protonation (see below). The titration

dx.doi.org/10.1021/jo201595s | J. Org. Chem. 2012, 77, 126−142

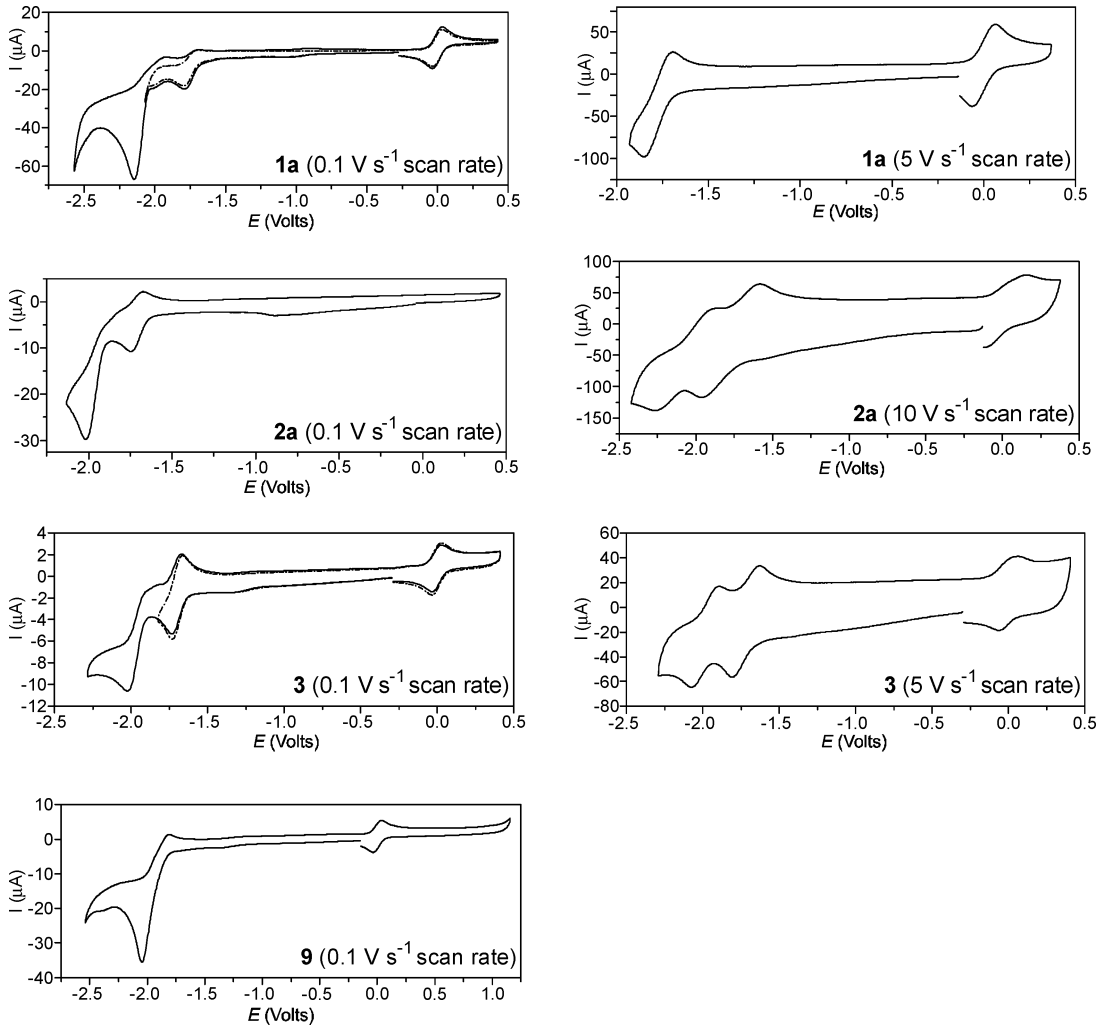

Figure 2. Cyclic voltammetry of **1a**, **2a**, **3**, and **9**. All CVs were recorded in CH_2Cl_2 with 0.1 mol/L $[(n\text{-}Bu_4)N]PF_6$, and the voltammograms were uncorrected for the Ohmic drop. The CV of **2a** at 0.1 V s^{-1} scan rate was performed in the absence of ferrocene and then calibrated to the ferrocene redox wave. All other CVs were recorded in the presence of ferrocene.

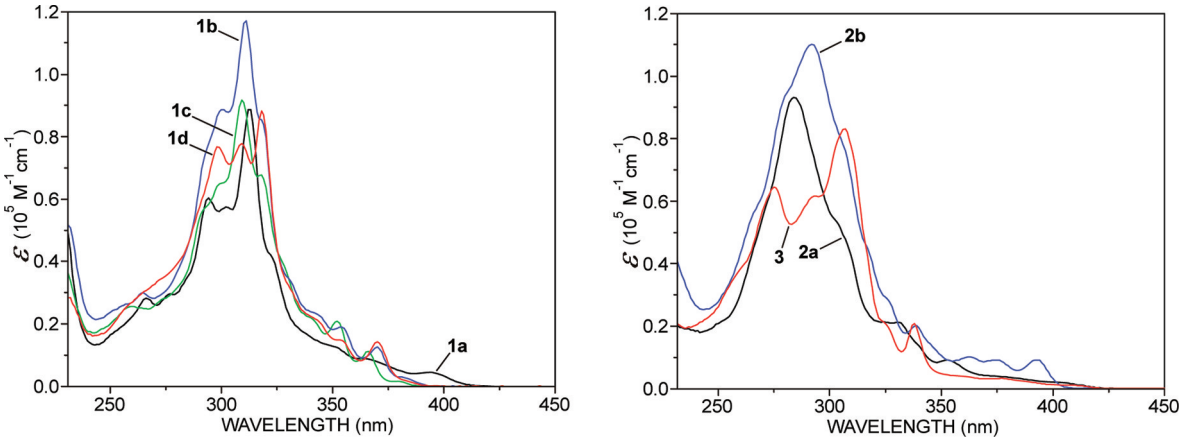

Figure 3. UV−vis absorption spectra of dehydrodipyrido[14]annulenes **1a−d** (left) and dehydro[*m*]pyrido[15]annulenes **2a,b** and **3** (right) recorded in CH_2Cl_2 solution.

experiment showed most noticeably that the coordination-induced changes in the UV−vis spectrum of **1a** occur over a large ligand:metal window; yet, a relatively high $[Hg^{II}]$ is required to induce a significant perturbation over the whole of the UV−vis of **1a** (Figure 5). On the basis of this latter experiment, we decided to use a 1:20 ratio of $[\mathbf{L}]$:$[Hg^{II}]$ for all subsequent **L**:Hg^{II} binding studies to ensure a significant spectroscopic response.

As in **1a**, the addition of Hg^{II} to **1b−d**, **2a,b**, and **3** results in a reduction in the absorption coefficient of the principle λ_{max} of

dx.doi.org/10.1021/jo201595s | J. Org. Chem. 2012, 77, 126−142

Table 2. UV−Vis and Luminescence Emission Spectroscopic Data for 1a−d, 2a,b, and 3

[m]pyrido[n]-annulene	no. [n]- π-electrons (no. [m] pyridine rings)	$\lambda_{abs\ solution}$ (nm)	$\lambda_{em\ solution}$ (nm)	$\lambda_{em\ thin\ film}$ (nm)	optical bandgap E_g^{opt} (eV)[a] (solution)	quantum yield Φ
1a	14 (2)	294, 302, 313[b]	411[b]	443,[b] 457sh	2.857 (3.037)	0.26
1b	14 (2)	300, 311,[b] 318sh	389,[b] 407, 422	421,[c] 432[c]	2.936 (3.157)	0.03
1c	14 (2)	299sh, 309,[b] 318	384,[b] 402, 418	411,[b,d] 428[d]	3.100 (3.195)	0.02
1d	14 (2)	299, 309, 318[b]	391,[b] 408,[b] 424sh	442	2.979 (3.169)	0.06
2a	15 (2)	284	429sh, 463[b]	501	2.731 (2.938)	0.06
2b	15 (2)	293	400,[b] 423, 437[b]	469	2.877 (3.076)	0.10
3	15 (3)	275, 293, 307[b]	421, 461[b]	525	2.732 (2.945)	0.04

[a]Optical bandgap extrapolated from the lowest energy absorption edge of drop-cast thin film UV−vis spectrum. Optical bandgap obtained from lowest energy absorption edge of CH_2Cl_2 solution UV−vis spectra in parentheses. [b]Highest intensity peaks. [c]Equal intensity peaks. [d]The relative intensity and line shape of these peaks vary according to the nature of the thin film and its angle with respect to the incident light. Unless otherwise stated, all UV−vis and luminescence solution measurements were performed in air-equilibrated CH_2Cl_2 at 20−25 °C.

the ligand, with an associated rise and extension to lower energy of the absorption tail (Figure 12 in the Supporting Information). Although the spectral response to Hg^{II} is relatively insensitive to isomer variations, it is dependent upon the number of π-electrons, being most pronounced for the dehydrodipyrido[14]annulenes **1a−d**.

In all cases, the addition of Hg^{II} at an [**L**]:[Hg^{II}] ratio of 1:20 (Figure 5) causes the luminescence λ_{max} to shift to lower energy, with the dehydrodipyrido[14]annulenes **1a−c** experiencing the greatest shifts.[94] The coordination-induced shifts of the pairs **1b**/**1c**, **1d**/**2b**, and **2a**/**3** are, however, strikingly similar, indicating a lower sensitivity to isomer differences. The similarity in the luminescence shifts of **2a** and **3** suggests that the central pyridine of **3** may have little involvement with Hg^{II} ion coordination in the excited state complex.

Spectroscopic Study of Protonation of 1a−d, 2a,b, and 3. Protonation of **4**−**6** resulted in a solution optical bandgap reduction as well as partial quenching and red-shifting of the luminescence, consistent with emission from aggregated excited states.[61] More recently, some donor-functionalized dehydrodipyrido[14]annulenes and dehydropyrido[15]-annulenes have also been shown to undergo various proton-induced shifts in the UV−vis and luminescence color changes.[75,76]

The effects of protonation on the UV−vis spectra of solutions of **1a−d**, **2a,b**, and **3** are shown in Figure 6 and in all cases show increased tailing of the low-energy absorption edge into the visible in the presence of 0.1 mol/L TFA. The proton-induced spectral shifts of the dehydro[m]pyrido[15]-annulenes **2a**−**3** involve λ_{max} red-shifting and moderate or zero reduction in molar absorption coefficients. The dehydrodipyrido[14]annulenes **1a−d** on the other hand experience more line shape rather than energy changes and significant molar absorption coefficient reductions, especially in the UV−vis of **1a**.

In contrast to the absorption changes, the solution luminescence spectra of **1a−d**, **2a,b**, and **3** undergo significant shifts in the λ_{max} to lower energy (by 46−101 nm) in the presence of 0.1 mol/L TFA (Figure 6). The sensitivity of the luminescence energy to acid was found to decrease in the following order: **1d** > **1a** ≅ **2b** > **2a** > **1c** > **1b** ≅ **3** and was accompanied by a range of visible color changes (Figure 7).

Cycles **1a** and **1d** are thus singular in their response to protonation, in both undergoing the largest UV−vis line shape changes and the strongest luminescence red-shifting. Overall, the proton-induced luminescence perturbations of **1a−d**, **2a,b**, and **3** are influenced by both the isomeric variations in nitrogen regiochemistry and the number of π-electrons.[95] However, further investigations such as, for example, time-resolved luminescence decay studies will be necessary to clearly characterize the emitting species generated upon protonation and Hg^{II} binding.

Finally, the visual distinction between protonation and Hg^{II} binding by **1a−d**, **2a,b**, and **3** is displayed more clearly as the collective response of all of the ligands in the form of a luminescence color pattern, rather than by the response of particular individual ligands. This observation raises the intriguing possibility that libraries of such ligands may find applications as luminescence fingerprint color sensors for particular metal ions.[96]

Quantum Mechanics Calculations. In contrast to the hydrocarbon annulenes and dehydroaryl[n]annulenes, dehydro[m]pyrido[n]annulenes are materials of comparatively recent existence and have consequently been little studied from a theoretical standpoint.[75,76,97,98] To obtain a deeper understanding of the electronic properties of **1a−d**, **2a,b**, and **3**, we therefore conducted a DFT investigation on these molecules using the Spartan 08 software[99] at the B3LYP level of theory and employing the 6-31G* basis set.[100,101]

Selected frontier molecular orbital (FMO) surfaces (**1a,b**, **2a**, and **3**) are shown in Figure 8 along with schematics for clarity, and those of **1c,d** and **2b** are in Figure 13 of the Supporting Information.[102] The dehydrodipyrido[14]annulenes **1b−d** exhibit similar highest occupied molecular orbitals (HOMOs), concentrated principally on the 1,4-di(pyridinyl)-buta-1,3-diyne units, whereas in **1a**, the HOMOs are nodal at the 1,4-buta-1,3-diyne bridge. However, the HOMOs on the nitrogens of **1a−c** are significantly contracted or nodal, suggesting that internitrogen electronic communication would be weak or negligible in the HOMOs of these systems. In contrast, the LUMOs of **1a**, **1c** and **1d** are almost identical and, in **1a** and **1d**, are concentrated on the pyridine nitrogens, the majority of the pyridine carbons and the 1,4-buta-1,3-diyne bridges, suggesting efficient internitrogen electronic communication in these molecules. The LUMO of **1b** on the other hand is located mainly on the nitrogens and 1,2-bis(pyridin-4-ylethynyl)benzene moiety, affording a "V"-shaped conjugation pathway suggestive of *ortho*-internitrogen electronic communication.

dx.doi.org/10.1021/jo201595s | J. Org. Chem. 2012, 77, 126−142

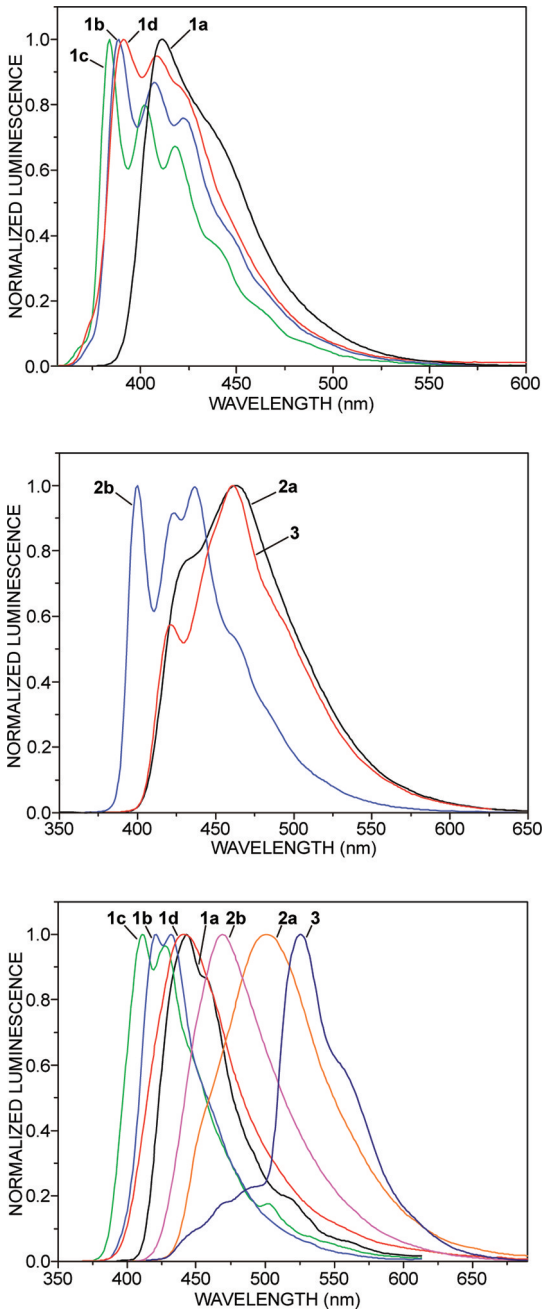

Figure 4. Normalized solution luminescence emission spectra of dehydrodipyrido[14]annulenes **1a–d** (upper), dehydro[*m*]pyrido-[15]annulenes **2a,b** and **3** (center), and drop-cast thin films of **1a–d**, **2a,b**, and **3** (lower). The solution luminescence emission spectra were recorded in CH_2Cl_2 solution (see the Supporting Information for experimental details).

The HOMOs of the dehydro[*m*]pyrido[15]annulenes **2a,b** and **3** are expanded on the pyridine nitrogens, the adjacent pyridine carbons, and the 1,4-buta-1,3-diyne bridges, indicating possible internitrogen electronic communication across these units. The LUMOs of **2a,b** and **3** are also similar to those of **1a**,**c**,**d** in being concentrated principally on the 1,4-di-(pyridinyl)buta-1,3-diyne units. This finding is in agreement with the site of reduction as indicated by the electrochemical measurements and suggestive of efficient internitrogen electronic communication in **2a,b** and **3**. However, in none of the FMOs of the dehydro[*m*]pyrido[14]- and [15]annulenes do we observe complete cyclic conjugation over the core of the macrocyclic ring.

Overall, **1a**, **2a**, and **3** exhibit LUMOs with *para*-connected orbital overlap between the pyridine nitrogens, which are additionally optimally positioned for external metal ion complexation. The generation of electro-reduced species or complexation to low oxidation state metals capable of electron donation into the LUMOs of these latter annulenes would thus be expected to achieve the most effective intermacrocyclic electronic communication within extended supramolecular arrays of dehydro[*m*]pyrido[*n*]annulenes.

The HOMO–LUMO energies and dipole moments of **1a–d**, **2a,b**, and **3** are given in Table 3. The calculated HOMO–LUMO bandgaps were all higher in energy than the optical bandgaps, with the closest agreement being between bandgaps estimated from solution UV–vis spectra and those calculated from the energy-minimized structures. The trend between experimental and calculated bandgaps was reasonable and in overall agreement within the limits of experimental error (Figure 14 in the Supporting Information).

Separation of the dehydro[*m*]pyrido[14]- and [15]annulenes into two groups as shown in Figure 9 revealed that within each group, the decrease in bandgaps upon passing, respectively, from **1c** to **1a** and **2b** to **2a** results principally from an increased relative reduction in the LUMO energy.

Thermochemical Properties. As high carbon content materials with an increased density of triple bonds are well-known to undergo topotactic[103] and amorphous carbonization polymerizations when heated,[104,105] we therefore considered it of interest to explore the thermochemical properties of our macrocycles. The TGA profiles of the dehydrodipyrido[14]- and [15]annulenes are shown in Figure 10, and all exhibited explosive decompositions at specific temperatures. However, no clear overall correlation between structure and thermal stability was observed. Wider investigations will therefore be necessary for general predictive structure–property relationships to emerge for these systems.

CONCLUSIONS

The above work discloses the synthesis of a range of isomeric parent dehydro[*m*]pyrido[14]- and [15]annulenes **1a–d**, **2a,b**, and **3**, which were characterized by NMR and mass spectroscopic techniques as well as crystallography in the case of **1b,c**. The macrocycles were found to function as luminescent chromophores in solution upon protonation and Hg^{II} coordination, with emissions sensitive to the number of π-electrons and isomeric composition of the macrocyclic ring. In the solid state, an even greater sensitivity to ligand structural characteristics as well as surrounding environment was evidenced by the observation of emission color-tuning. In particular, the ion-specific luminescence color patterns that collectively result from the differing spectroscopic isomer responses suggest potential applications as "fingerprint" analyte sensors.

Ligand **1a** afforded a unique spectroscopic profile in being a relatively low optical bandgap material, which shared the strongest Hg^{II} and proton-induced emission energy changes and molar absorption coefficient perturbations within the dehydro[*m*]pyrido[14]- and [15]annulene series. It also exhibits the highest luminescence quantum yield.

The DFT calculations corroborated the spectroscopic findings that **1a**, **2a**, and **3** are the lowest bandgap materials with LUMOs delocalized over the *para*-connected pyridine rings and intervening 1,4-buta-1,3-diyne bridges, a conclusion

dx.doi.org/10.1021/jo201595s | *J. Org. Chem.* 2012, 77, 126–142

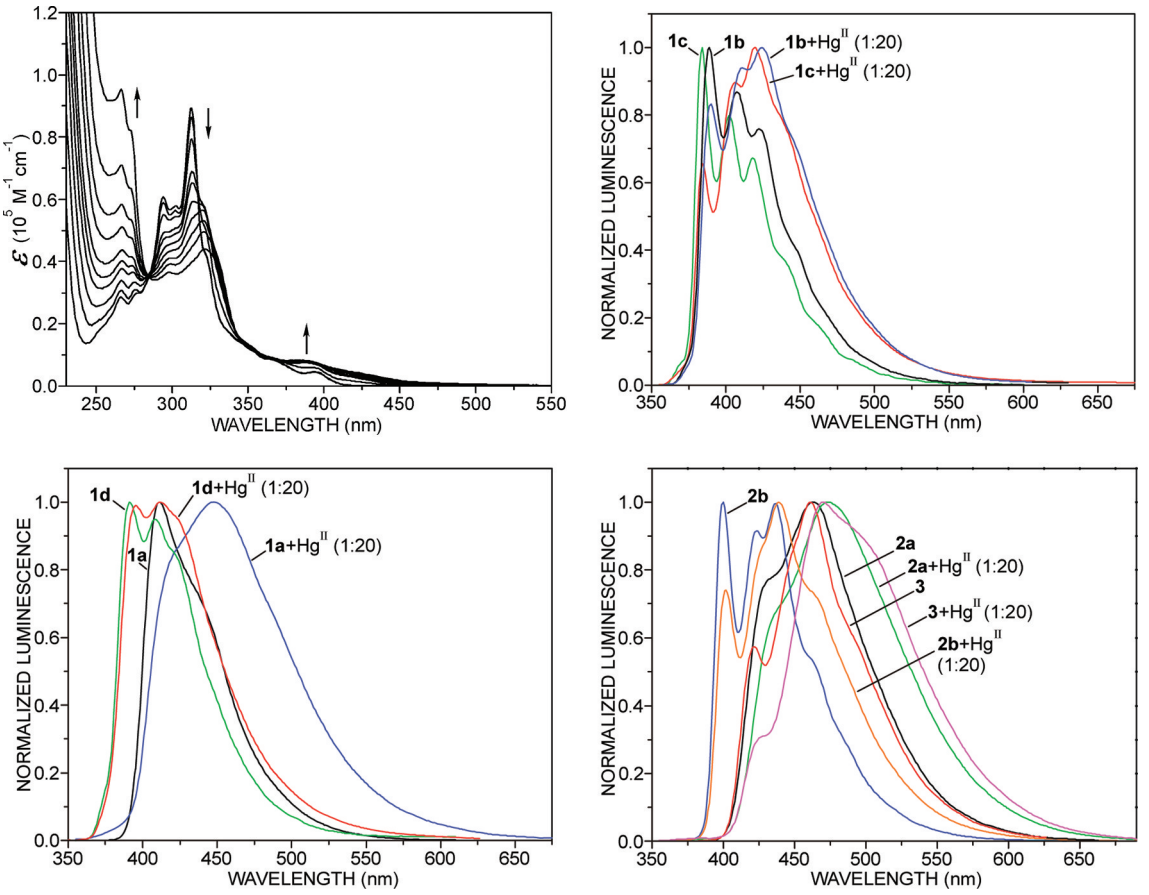

Figure 5. UV−vis absorption spectra of **1a** titrated with incremental additions of $Hg(CF_3SO_3)_2$ (upper left), where the [**1a**]:[Hg^{II}] ratios are, respectively, 1:0, 1:4, 1:8, 1:12, 1:16, 1:20, 1:30, 1:40, 1:60, and 1:100, recorded 40 h after solution preparation. Normalized luminescence emission spectra of **1b** and **1c** (**L**) (upper right), **1a** and **1d** (**L**) (lower left), and **2a**,**b** and **3** (**L**) (lower right) with $Hg(CF_3SO_3)_2$; [**L**]:[Hg^{II}] ratio = 1: 20; spectra recorded 7 days after solution preparation. All **L** + Hg^{II} spectra were recorded in 10% $MeOH/CH_2Cl_2$, and those of pure **L** were recorded in CH_2Cl_2.

supported by the electrochemical measurements that showed reduction to be insensitive to the nature of the 1,3-aromatic bridge in **2a** and **3**. Isomeric variation within the dehydro[*m*]-pyrido[14]- and [15]annulenes clearly also results in bandgap fine-tuning. The superior LUMO delocalization between the pyridine nitrogens along with their *para*-connectivity and ideal regiochemistry leads to the anticipation that **1a**, **2a**, and **3** would be the most suitable candidates for the assembly of electronically delocalized supramolecular arrays and polymers, when complexed to low oxidation state metals capable of back-donation of electrons into the ligand π^* LUMOs.

Furthermore, the finding that cyclization of the 1,4-di(pyridin-4-yl)buta-1,3-diyne unit results in augmented monoanion radical stabilization upon reduction as well as optical bandgap lowering and improved electronic delocalization as compared to acyclic analogues suggests that the development of molecular solenoids and hybrid nanoelectronic materials with curved electronic pathways based upon the optimally conjugated *para*-arylethynylenes is viable.[106,107] Work towards this goal along with the creation of hybrid dehydro[*m*]pyrido[*n*]annulene-coordination polymers based upon **1a** are currently in progress.

EXPERIMENTAL SECTION

The general experiment is described in the Supporting Information.

Synthetic Procedures and Characterization Data for 1a−d, 2a,b, 3, 12a−d, 13a−d, 15−17, 19a,b, 20a,b, 22, and 23. Variations in the following procedures A−C were necessary in some cases to achieve optimal product yields and purities. These details are provided below when necessary for the particular products concerned. Slow heating of **1a−d**, **2a,b**, **3**, **13a−d**, **20a,b**, and **23** at 1−2 °C/min up to 310 °C resulted in a gradual color change to black, with no visible melting phase.

A. Sonogashira Type Heterocouplings. To the respective arylalkyne and $PdCl_2(PPh_3)_2$ catalyst under an atmosphere of argon was added N_2-purged Et_3N followed by the appropriate quantity of diiodobenzene consecutively by syringe. After it was stirred for 0.2 h, a solution of CuI in N_2-purged Et_3N (prepared in a separate Schlenk under argon) was syringed into the reaction, and stirring was continued for 4−21 days at ambient temperature in the absence of light. A pale dark gray or brown precipitate slowly formed in all cases, visually indicating the progress of the reaction. All solvent was then removed under reduced pressure in a water bath at 70 °C, and the residue was extracted with 5 × 30 mL of pentane. The combined extracts were gravity filtered, and the solvent was removed under reduced pressure on a water bath at ambient temperature. The crude product was purified as described individually for each compound below. As the reaction conditions and yields of the Sonogashira couplings were not optimized, the reactions were run with an emphasis on longer rather than shorter reaction times to ensure complete conversion of the starting materials.

B. Fluoride-Mediated Desilylations. To a stirred solution of the triisopropylsilylalkyne in THF was first added dropwise a small quantity of distilled water followed by the appropriate quantity of the $[(n\text{-}Bu)_4N]F$ (1.0 M in THF) solution, and stirring was continued at ambient temperature in the absence of light until TLC sampling indicated complete deprotection (1−4 days). The reaction was

dx.doi.org/10.1021/jo201595s | J. Org. Chem. 2012, 77, 126−142

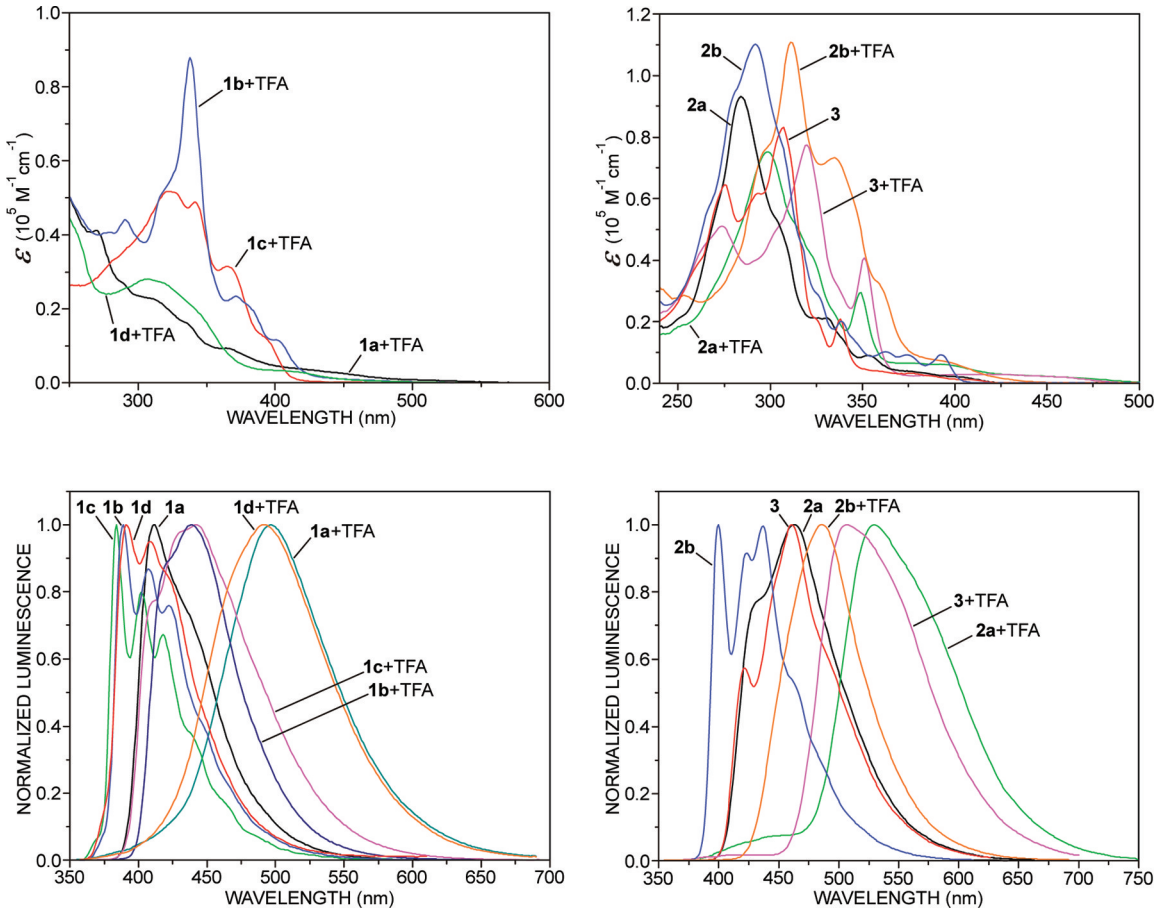

Figure 6. UV−visible absorption spectra of **1a−d** (upper left) and **2a,b** and **3** (**L**) (upper right) in CH_2Cl_2/TFA ([TFA] = 0.1 mol/L) with **2a,b** and **3** in pure CH_2Cl_2 for comparison in the upper right spectrum. Normalized luminescence emission spectra of **1a−c** (lower left) and **2a,b** and **3** (lower right) in CH_2Cl_2/TFA ([TFA] = 0.1 mol/L) and in pure CH_2Cl_2 for comparison. [**L**] = 7−9 × 10^{-6} mol/L.

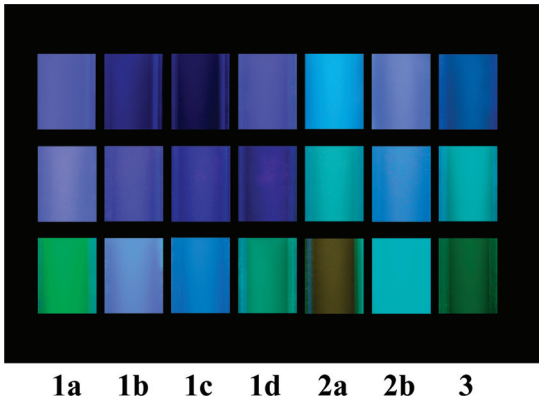

Figure 7. From left to right: solutions of **1a−d**, **2a,b**, and **3** (**L**) with [**L**] = 7−9 × 10^{-6} mol/L; in CH_2Cl_2 (upper), in 10% MeOH/CH_2Cl_2 with a 1:20 ratio of [**L**]:[Hg^{II}] (center), and in 0.1 mol/L TFA in CH_2Cl_2 (bottom row), under illumination by a high intensity 312 nm UV lamp in the dark.

quenched by the addition of distilled water, and all solvent was removed under reduced pressure at ambient temperature. The crude product was purified as described individually for each compound below.

C. Macrocyclizations (Eglinton/Galbraith Protocol). In a well-ventilated hood, a solution of the dialkyne in toluene was added dropwise over 0.7−2.5 h to a solution of anhydrous Cu_2OAc_4 in pyridine (400−567 mL) with rapid stirring at 55 °C. After the addition of the dialkyne was complete, the reaction was stirred for a further 0.25−1 h, and then, all solvent was removed under reduced pressure on a water bath at 40 °C. The residue was further dried in a stream of air and then distilled water (200−300 mL) added, followed by excess ice, and the mixture vigorously stirred. Excess solid KCN (4−5 g) was then added in portions with continued stirring, until no further visible change occurred, at which point the mixture appeared as a brown suspension. Further workup and purification methods are detailed separately for each product below.

Macrocycles **1a−d**, **2a,b**, and **3** were isolated as described below with ≤1 mol % entrained CH_2Cl_2 after air-drying, as judged by the ^1H NMR integrations. The entrained solvent could be removed upon heating to 85−95 °C in a gentle stream of argon for 0.5 h.

1,2-Bis((4-((triisopropylsilyl)ethynyl)pyridin-3-yl)ethynyl)-benzene (12a). According to general procedure A, **10a** (0.788 g, 2.78 × 10^{-3} mol), **11** (0.400 g, 1.21 × 10^{-3} mol), and $PdCl_2(PPh_3)_2$ (0.068 g, 9.69 × 10^{-5} mol) in Et_3N (20 mL), to which was added a solution of CuI (0.053 g, 2.78 × 10^{-4} mol) in Et_3N (10 mL), was stirred for 4 days and worked up to yield crude **12a**. The product was then chromatographed on a column of neutral alumina (activity II/III) eluting first with CH_2Cl_2 to remove some less polar impurities. The column was subsequently gradient eluted with 1−5% MeOH/CH_2Cl_2 to obtain the product, which was isolated as pale honey-colored oil that solidified into a tacky glass upon standing for several weeks. Further drying under vacuum at 70−80 °C/0.001 mm Hg was necessary to remove residual CH_2Cl_2 to yield pure **12a** (0.754 g, 97%). ^1H NMR ($CDCl_3$, 400.13 MHz, 23 °C): δ 8.710 (d, $^5J(2,5)$ = 0.9 Hz, 2H; pyH2), 8.454 (d, $^3J(6,5)$ = 5.1 Hz, 2H; pyH6), 7.567 (m, 2H; phH3/6), 7.346 (m, 2H; phH4/5), 7.344 (dd, $^3J(5,6)$ = 5.1 Hz, $^5J(5,2)$ = 0.8 Hz, 2H; pyH5), 1.091 (m, 42H; $CH(CH_3)_2$). ^{13}C NMR

dx.doi.org/10.1021/jo201595s | J. Org. Chem. 2012, 77, 126−142

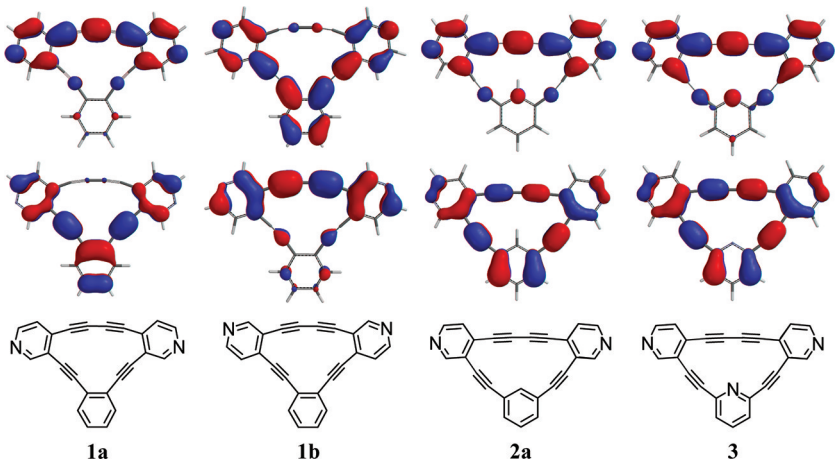

Figure 8. FMOs (B3LYP/6-31G*) of **1a,b**, **2a**, and **3**. LUMO (upper) and HOMO (lower) plots, with molecular schematics shown at the bottom.

Table 3. Energy Properties and Dipole Moments Calculated (B3LYP/6-31G*) for 1a–d, 2a,b, and 3 in the Gas Phase

annulene	*E* (HOMO) (eV)	*E* (LUMO) (eV)	Δ*E* (L–H) (eV)	*μ* (D)
1a	−6.014	−2.484	3.529	0.59
1b	−5.965	−2.332	3.633	5.41
1c	−5.818	−2.112	3.706	1.46
1d	−5.894	−2.193	3.701	5.92
2a	−5.970	−2.637	3.333	0.09
2b	−5.927	−2.425	3.502	4.35
3	−5.976	−2.601	3.374	1.13

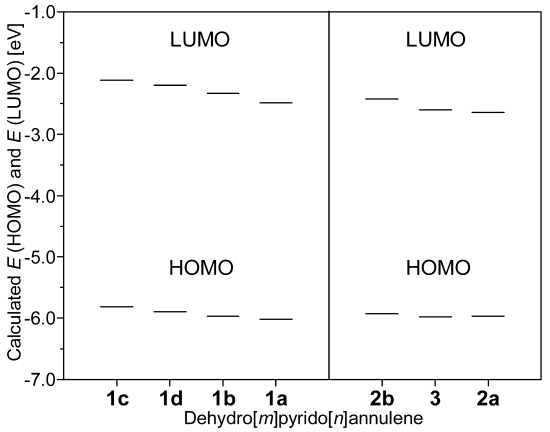

Figure 9. HOMO and LUMO energies (B3LYP/6-31G*) of **1a–d**, **2a,b**, and **3** as a function of annulene structure.

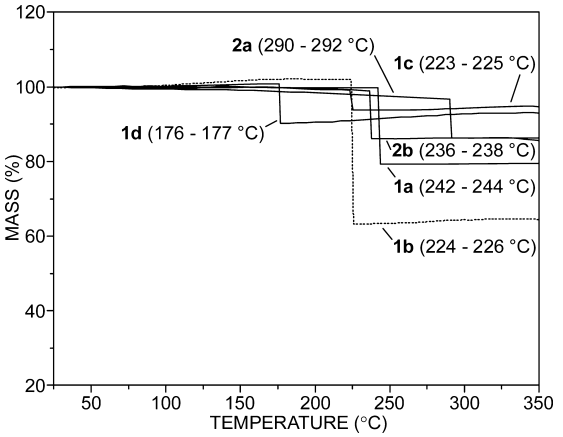

Figure 10. TGA thermal decomposition profiles of **1a–d**, **2a**, and **2b**, heated at a rate of 10 °C/min under an inert atmosphere. The decomposition temperature ranges are shown in brackets for the respective dehydrodipyrido[14]- and [15]annulenes.

($CDCl_3$, 100.61 MHz, 23 °C): δ 152.8, 148.2, 132.9, 132.0, 128.4, 125.8, 125.5, 121.8, 102.6 (−C≡), 101.3 (−C≡), 94.3 (−C≡), 89.5 (−C≡), 18.6 ($CH(CH_3)_2$), 11.2 ($CH(CH_3)_2$). IR (thin film): 2941 (s), 2891 (m), 2864 (s), 1574 (s), 1488 (s), 1462 (s), 1398 (s), 1164 (m), 996 (s), 882 (s), 865 (s), 828 (s), 802 (s), 755 (s), 677 (s), 663 (s), 641 cm^{-1} (s). High res. ESI MS: *m/z* (%): 641.3658 (100) [*M* + H^+]. Calcd for $C_{42}H_{53}N_2Si_2$, 641.3742.

1,2-Bis((4-ethynylpyridin-3-yl)ethynyl)benzene (13a). Compound **13a** was obtained from the reaction of **12a** (0.730 g, 1.14 × 10^{-3} mol) with [(*n*-Bu)$_4$N]F (1.0 M in THF; 2.4 mL, 2.4 × 10^{-3} mol) in THF (60 mL) to which 10 drops of H_2O had been added, after 1 day according to the general deprotection procedure B. Methanol (20 mL) was added to the residue, the mixture was filtered under vacuum, and the isolated solid was washed with excess methanol and air-dried. The solvent was removed from the filtrate under reduced pressure at ambient temperature to yield a dark oil, which was chromatographed on neutral alumina (activity III), eluting with CH_2Cl_2. Pentane (15 mL) was added, and the mixture briefly ultrasonicated. The crystalline solid that formed, was isolated by filtration under vacuum, washed with pentane (4 × 0.5 mL) and air-dried. This latter solid was combined with the solid obtained from the methanol washing of the crude product above and dissolved in boiling heptane (150 mL) to which 0.1 g of NORIT A had been added. After it was heated for 1 min, the mixture was gravity filtered and left to cool to ambient temperature in the dark. The crystalline solid that formed was isolated by filtration under vacuum, washed with heptane (4 × 1 mL), and air-dried to afford **13a** (0.299 g, 80%) as cream-colored microflakes. ^{1}H NMR ($CDCl_3$, 400.13 MHz, 25 °C): δ 8.802 (d, ^5J(2,5) = 0.5 Hz, 2H; pyH2), 8.510 (d, ^3J(6,5) = 5.3 Hz, 2H; pyH6), 7.645 (m, 2H; phH3/6), 7.392 (m, 2H; phH4/5), 7.383 (d, ^3J(5,6) = 4.8 Hz, 2H; pyH5), 3.421 (s, 2H; −C≡CH). ^{13}C NMR ($CDCl_3$, 100.61 MHz, 25 °C): δ 152.7, 148.3, 132.5, 131.9, 128.8, 125.8, 125.0, 122.2, 94.7 (−C≡), 88.8 (−C≡), 85.9 (−C≡), 79.6 (−C≡). UV–vis (CH_2Cl_2): λ_{max} (ε) = 239 (5.4 × 10^4), 280 (2.9 × 10^4), 313 (2.5 × 10^4), 326sh (2.3 × 10^4), 336 nm; sh (2.1 × 10^4 M^{-1} cm^{-1}). IR (thin film): 3284 (s) (≡C–H), 3187 (s) (≡C–H), 3055 (w), 2106 (s) (C≡C), 1577 (s), 1487 (s), 1443 (s), 1399 (s), 1049 (s), 849 (s), 837 (vs), 759 (vs), 753 (vs), 694 (s), 641 cm^{-1} (s). High res. ESI MS: *m/z* (%): 329.1062 (100) [*M* + H^+], 335.1159 (27) [*M* + Li^+], 351.0906 (4) [*M* + Na^+], 663.2068 (9) [2*M* + Li^+]. Calcd for $C_{24}H_{13}N_2$, 329.1073; $C_{24}H_{12}LiN_2$, 335.1155; $C_{24}H_{12}NaN_2$, 351.0893; $C_{48}H_{24}LiN_4$, 663.2156.

dx.doi.org/10.1021/jo201595s | *J. Org. Chem.* 2012, 77, 126–142

Dehydro[2]pyrido[14]annulene (1a) via Copper-Mediated Cyclization of 13a. A solution of **13a** (0.060 g, 1.83×10^{-4} mol) in toluene (30 mL) was added to a stirred solution of anhydrous Cu_2OAc_4 (1.330 g, 3.66×10^{-3} mol) in pyridine (400 mL) at 55 °C over 2 h. The reaction was stirred at the above temperature for a further 0.5 h, and then, the reaction worked up as described in the general macrocyclization procedure C. The straw-colored aqueous KCN suspension was extracted with CH_2Cl_2 (3 × 60 mL), the combined extracts were dried (anhydrous Na_2SO_4) and gravity filtered, and the solvent was reduced in volume to 20 mL under reduced pressure at ambient temperature. The concentrate was chromatographed first on a column of basic alumina (activity IV) and then on a short column of neutral alumina (activity III) in complete darkness, in both cases eluting with CH_2Cl_2. The solvent was removed under vacuum at ambient temperature in darkness, and the remaining solid was suspended in MeCN (10 mL), briefly ultrasonicated, isolated by filtration under vacuum, washed with MeCN (3 × 1 mL), and air-dried at ambient temperature to constant mass affording **1a** (0.040 g, 67%) as a fibrous cream-colored solid. ^{1}H NMR ($CDCl_3$, 400.13 MHz, 24 °C): δ 9.129 (d, ^5J(2,5) = 0.8 Hz, 2H; pyH2), 8.669 (d, ^3J(6,5) = 5.1 Hz, 2H; pyH6), 7.972 (m, 2H; phH3/6), 7.541 (m, 2H; phH4/5), 7.458 (dd, ^3J(5,6) = 5.1 Hz, ^5J(5,2) = 0.7 Hz, 2H; pyH5). ^{13}C NMR ($CDCl_3$, 100.61 MHz, 26 °C): δ 153.2, 147.9, 136.1, 129.4, 128.7, 125.4, 122.9, 122.1, 96.6 (−C≡), 89.9 (−C≡), 84.9 (−C≡), 83.5 (−C≡). UV−vis (CH_2Cl_2): λ_{max} (ε) = 266 (2.8×10^4), 277 (3.0×10^4), 294 (6.0×10^4), 302 (5.7×10^4), 313 (8.9×10^4), 323sh (4.1×10^4), 352 (1.2×10^4), 362 (8.9×10^3), 394 nm (4.5×10^3 M^{-1} cm^{-1}). IR: 3041 (w), 3025 (w), 2181 (w) (C≡C), 2162 (w) (C≡C), 1573 (m), 1476 (m), 1406 (m), 1272 (m), 1255 (m), 878 (m), 829 (s), 792 (m), 754 (vs), 748 (s), 597 cm^{-1} (m). High res. ESI MS: m/z (%): 327.0883 (88) [M + H^+], 333.0969 (100) [M + Li^+], 659.1717 (7) [2M + Li^+]. Calcd for $C_{24}H_{11}N_2$, 327.0917; $C_{24}H_{10}LiN_2$, 333.0999; $C_{48}H_{20}LiN_4$, 659.1843.

Dehydro[2]pyrido[14]annulene (1a) via Palladium-Mediated Cyclization of 13a. A mixture of $PdCl_2$(dppe) (0.018 g, 3.1×10^{-5} mol), CuI (0.09 g, 5×10^{-5} mol), and iodine (0.039 g, 3.1×10^{-4} mol) in 1:1 THF/i-Pr_2NH (600 mL) was homogenized by brief ultrasonication and stirred at 50 °C for 0.5 h. A solution of **13a** (0.100 g, 3.0×10^{-4} mol) in THF (20 mL) was then added to the warm catalyst mixture dropwise over 9 h with vigorous stirring. The reaction was stirred at the above temperature for a further 1 h, and all solvent subsequently was removed under reduced pressure at 30 °C. The residue was treated with aqueous KCN as described in the general procedure C and purified as described above for the copper-mediated cyclization of **13a** to afford **1a** (0.023 g, 23%).

1,2-Bis((3-((triisopropylsilyl)ethynyl)pyridin-4-yl)ethynyl)-benzene (12b). According to general procedure A, **10b** (0.600 g, 2.12×10^{-3} mol), **11** (0.350 g, 1.06×10^{-3} mol), and $PdCl_2(PPh_3)_2$ (0.100 g, 1.42×10^{-4} mol) in Et_3N (30 mL), to which was added a solution of CuI (0.100 g, 5.25×10^{-4} mol) in Et_3N (6 mL), were stirred for 21 days and worked up to yield crude **12b**. The product was then purified by column chromatography three times on neutral alumina (activity III), eluting with CH_2Cl_2. After the solvent was removed by distillation on a water bath, the product was air dried to yield pure **12b** (0.470 g, 69%) as a pale honey-colored oil. ^{1}H NMR ($CDCl_3$, 400.13 MHz, 25 °C): δ 8.735 (d, ^5J(2,5) = 0.7 Hz, 2H; pyH2), 8.441(d, ^3J(6,5) = 5.3 Hz, 2H; pyH6), 7.581 (m, 2H; phH3/6), 7.382 (m, 2H; phH4/5), 7.320 (dd, ^3J(5,6) = 5.2 Hz, ^5J(5,2) = 0.8 Hz, 2H; pyH5), 1.103 (m, 42H; $CH(CH_3)_2$). ^{13}C NMR ($CDCl_3$, 100.61 MHz, 25 °C): δ 153.3, 148.0, 133.0, 132.1, 128.8, 125.3, 125.2, 121.7, 102.0 (−C≡), 99.2 (−C≡), 95.8 (−C≡), 90.1 (−C≡), 18.6 ($CH(CH_3)_2$), 11.2 ($CH(CH_3)_2$). IR (thin film): 2941 (s), 2890 (m), 2863 (s), 2223 (w) (C≡C), 2155 (w) (C≡C), 1575 (s), 1462 (s), 1398 (s), 1283 (m), 1185 (m), 996 (m), 882 (s), 826 (s), 803 (s), 756 (s), 669 cm^{-1} (s). High res. ESI MS: m/z (%): 641.3736 (100) [M + H^+]. Calcd for $C_{42}H_{53}N_2Si_2$, 641.3742.

1,2-Bis((3-ethynylpyridin-4-yl)ethynyl)benzene (13b). Compound **13b** was obtained from the reaction of **12b** (0.400 g, 6.24×10^{-4} mol) with [(n-Bu)$_4$N]F (1.0 M in THF; 2.0 mL, 2.0×10^{-3} mol) in THF (25 mL) to which 1 mL of H_2O had been added, after 2 days according to the general deprotection procedure B. The residue that remained upon removal of the solvent was partitioned between water (350 mL) and CH_2Cl_2 (60 mL) and extracted with a further 60 mL aliquot of CH_2Cl_2. The combined organic extracts were further extracted with water, then dried (anhydrous Na_2SO_4), and gravity filtered, and the solvent was removed under reduced pressure at ambient temperature. The remaining solid was boiled in 600 mL of Et_2O and gravity filtered, and the Et_2O was distilled off on a water bath. The product was finally dissolved in 40 mL of boiling heptane to which 0.1 g of NORIT A had been added, gravity filtered, and left to stand in the dark for 1 day. The solid that formed was isolated by vacuum filtration, washed with heptane, and air-dried to yield **13b** (0.140 g, 68%) as cream microcrystals. ^{1}H NMR ($CDCl_3$, 400.13 MHz, 25 °C): δ 8.767 (d, ^5J(2,5) = 0.7 Hz, 2H; pyH2), 8.543 (d, ^3J(6,5) = 5.1 Hz, 2H; pyH6), 7.661 (m, 2H; phH3/6), 7.427 (m, 2H; phH4/5), 7.408 (dd, ^3J(5,6) = 5.2 Hz, ^5J(5,2) = 0.8 Hz, 2H; pyH5), 3.343 (s, 2H; −C≡CH). ^{13}C NMR ($CDCl_3$, 100.61 MHz, 31 °C): δ 153.2, 148.7, 133.6, 132.8, 129.2, 125.2, 124.8, 120.6, 96.1 (−C≡), 89.5 (−C≡), 84.3 (−C≡), 79.1 (−C≡). UV−vis (CH_2Cl_2): λ_{max} (ε) = 228 (4.9×10^4), 242 (4.8×10^4), 290 (3.6×10^4), 309 (2.4×10^4), 317sh (2.4×10^4), 330 nm; sh (2.1×10^4 M^{-1} cm^{-1}). IR (thin film): 3301 (m) (≡C−H), 3155 (m) (≡C−H), 2222 (m) (C≡C), 2204 (m) (C≡C), 2098 (m) (C≡C), 1577 (vs), 1495 (m), 1442 (m), 1400 (s), 855 (m), 832 (vs), 758 (vs), 708 (s), 673 (s), 646 (s), 624 cm^{-1} (vs). High res. ESI MS: m/z (%): 329.1066 (100) [M + H^+]. Calcd for $C_{24}H_{13}N_2$, 329.1073. Anal. (%) calcd for $C_{24}H_{12}N_2$: C, 87.79; H, 3.68; N, 8.53. Found: C, 87.45; H, 3.65; N, 8.44.

Dehydro[2]pyrido[14]annulene (1b). A solution of **13b** (0.076 g, 2.31×10^{-4} mol) in toluene (30 mL) was added dropwise to a stirred solution of anhydrous Cu_2OAc_4 (1.682 g, 4.63×10^{-3} mol) in pyridine (507 mL) at 55 °C over 2.25 h. The reaction was stirred at the above temperature for a further 0.3 h, and then, the reaction was worked up as described in the general macrocyclization procedure C. The aqueous KCN suspension was filtered under vacuum, and the isolated straw-colored solid was washed with excess distilled water and air-dried. The solid was then dissolved in CH_2Cl_2 (20 mL) and chromatographed on a column of basic alumina (activity IV), which was completely shielded from the light, eluting with CH_2Cl_2. The solvent was removed under vacuum from the eluate containing **1b**, at ambient temperature in darkness. The remaining solid was suspended in MeCN (10 mL), briefly ultrasonicated, isolated by filtration under vacuum, washed with MeCN (4 × 1 mL), and air-dried at ambient temperature to a constant mass affording **1b** (0.070 g, 93%) as a cream microcrystalline solid. ^{1}H NMR ($CDCl_3$, 400.13 MHz, 24 °C): δ 8.866 (d, ^5J(2,5) = 0.7 Hz, 2H; pyH2), 8.696 (d, ^3J(6,5) = 5.3 Hz, 2H; pyH6), 7.961 (m, 2H; phH3/6), 7.722 (dd, ^3J(5,6) = 5.2 Hz, ^5J(5,2) = 0.8 Hz, 2H; pyH5), 7.560 (m, 2H; phH4/5). ^{13}C NMR ($CDCl_3$, 100.61 MHz, 25 °C): δ 149.9, 148.6, 136.7, 136.6, 129.2, 126.0, 122.9, 118.5, 97.7 (−C≡), 90.7 (−C≡), 84.4 (−C≡), 83.2 (−C≡). UV−vis (CH_2Cl_2): λ_{max} (ε) = 265 (3.0×10^4), 300 (8.9×10^4), 311 (1.2×10^5), 318sh (8.5×10^4), 343sh (2.3×10^4), 353 (1.9×10^4), 370 (1.3×10^4), 383 nm (2.7×10^3 M^{-1} cm^{-1}). IR: 3036 (w), 2182 (m) (C≡C), 2160 (vw) (C≡C), 1577 (m), 1518 (m), 1496 (m), 1476 (m), 1418 (m), 1400 (m), 1272 (m), 1165 (m), 954 (m), 882 (m), 838 (s), 753 (vs), 746 (s), 710 (m), 586 (m), 580 (s), 576 cm^{-1} (s). EI MS m/z (%): 326.0 (100) [M^+]. High res. ESI MS: m/z (%): 327.0909 (100) [M + H^+]. Calcd for $C_{24}H_{11}N_2$, 327.0917.

1,2-Bis((3-((triisopropylsilyl)ethynyl)pyridin-2-yl)ethynyl)-benzene (12c). According to general procedure A, **10c** (0.729 g, 2.57×10^{-3} mol), **11** (0.362 g, 1.10×10^{-3} mol), and $PdCl_2(PPh_3)_2$ (0.050 g, 7.12×10^{-5} mol) in Et_3N (20 mL), to which was added a solution of CuI (0.050 g, 2.63×10^{-4} mol) in Et_3N (10 mL), was stirred for 21 days, and worked up to yield crude **12c**. The product was then chromatographed twice on neutral alumina (activity III), eluting in both cases with CH_2Cl_2. The product thus obtained was stirred briefly in 30 mL of Et_2O to which 0.560 g of NORIT A had been added and then gravity filtered, and the solvent was distilled off at atmospheric pressure on a water bath. Drying under vacuum at 70 °C/0.001 mm Hg removed the last traces of Et_2O to yield **12c** (0.491 g, 70%) as a pale honey-colored glass. ^{1}H NMR ($CDCl_3$, 400.13 MHz, 28 °C): δ 8.489 (dd, ^3J(6,5) = 4.8 Hz, ^4J(6,4) = 1.7 Hz, 2H; pyH6),

dx.doi.org/10.1021/jo201595s | J. Org. Chem. 2012, 77, 126−142

7.759 (dd, $^3J(4,5)$ = 7.9 Hz, $^4J(4,6)$ = 1.8 Hz, 2H; pyH4), 7.613 (m, 2H; phH3/6), 7.323 (m, 2H; phH4/5), 7.153 (dd, $^3J(5,4)$ = 7.9 Hz, $^3J(5,6)$ = 4.9 Hz, 2H; pyH5), 1.078 (m, 42H; $CH(CH_3)_2$). ^{13}C NMR ($CDCl_3$, 100.61 MHz, 28 °C): δ 148.6, 144.9, 139.8, 132.9, 128.2, 125.2, 123.1, 121.8, 102.9 (−C≡), 98.5 (−C≡), 91.8 (−C≡), 90.9 (−C≡), 18.6 ($CH(CH_3)_2$), 11.3 ($CH(CH_3)_2$). IR (thin film): 2942 (s), 2891 (m), 2864 (s), 2222 (w) (C≡C), 2157 (w) (C≡C), 1462 (m), 1445 (m), 1416 (s), 1199 (m), 1097 (m), 993 (m), 882 (s), 797 (vs), 765 (vs), 752 (s), 678 (vs), 658 (vs), 639 (vs), 637 (vs), 628 cm^{-1} (vs). High res. ESI MS: *m/z* (%): 641.3782 (100) [*M* + H^+], 647.3921 (30) [*M* + Li^+], 663.3600 (50) [*M* + Na^+], 679.3353 (11) [*M* + K^+]. Calcd for $C_{42}H_{53}N_2Si_2$, 641.3742; $C_{42}H_{52}LiN_2Si_2$, 647.3824; $C_{42}H_{52}N_2NaSi_2$, 663.3561; $C_{42}H_{52}KN_2Si_2$, 679.3301.

1,2-Bis((3-ethynylpyridin-2-yl)ethynyl)benzene (13c). According to the general deprotection procedure B, **12c** (0.459 g, 7.16 × 10^{-4} mol) in THF (80 mL) to which 10 drops of H_2O had been added, with [(*n*-Bu)$_4$N]F (1.0 M in THF; 1.5 mL, 1.5 × 10^{-3} mol), was stirred for 1 day at ambient temperature. A second aliquot of [(*n*-Bu)$_4$N]F (1.5 mL) was added, and stirring was continued for a further 12 h. The residue that remained after removal of the solvent was partitioned between water (160 mL) and Et_2O (120 mL), and the aqueous layer was extracted with a further 2 × 40 mL of Et_2O. The combined organic extracts were further extracted with 4 × 80 mL of water, then dried (anhydrous Na_2SO_4), and gravity filtered, and the solvent was removed under reduced pressure at ambient temperature. The product was then chromatographed on neutral alumina (activity III) eluting with CH_2Cl_2 to yield a pale honey-colored glass after removal of the solvent by distillation on a water bath and drying under vacuum. The glass was recrystallized from heptane and air-dried to afford **13c** (0.200 g, 85%) as colorless needles. ^1H NMR ($CDCl_3$, 400.13 MHz, 26 °C): δ 8.571 (dd, $^3J(6,5)$ = 4.8 Hz, $^4J(6,4)$ = 1.7 Hz, 2H; pyH6), 7.788 (dd, $^3J(4,5)$ = 7.9 Hz, $^4J(4,6)$ = 1.7 Hz, 2H; pyH4), 7.716 (m, 2H; phH3/6), 7.383 (m, 2H; phH4/5), 7.211 (dd, $^3J(5,4)$ = 7.9 Hz, $^3J(5,6)$ = 4.9 Hz, 2H; pyH5), 3.560 (s, 2H; −C≡CH). ^{13}C NMR ($CDCl_3$, 100.61 MHz, 26 °C): δ 149.0, 145.7, 139.5, 133.5, 128.9, 124.8, 122.4, 122.0, 91.7 (−C≡), 91.3 (−C≡), 85.0 (−C≡), 79.7 (−C≡). UV−vis (CH_2Cl_2): λ_{max} (ε) = 229 (4.0 × 10^4), 244 (4.1 × 10^4), 287 (2.7 × 10^4), 306 (2.2 × 10^4), 328 (2.1 × 10^4), 349 nm; sh (1.0 × 10^4 M^{-1} cm^{-1}). IR (thin film): 3274 (s) (≡C−H), 3170 (s) (≡C−H), 3053 (m), 2217 (m) (C≡C), 2102 (m) (C≡C), 1549 (s), 1489 (s), 1447 (s), 1440 (s), 1414 (vs), 1093 (s), 1090 (s), 801 (vs), 760 (vs), 723 (vs), 671 (vs), 646 cm^{-1} (vs). High res. ESI MS: *m/z* (%): 329.1059 (100) [*M* + H^+], 335.1138 (74) [*M* + Li^+], 351.0874 (13) [*M* + Na^+]. Calcd for $C_{24}H_{13}N_2$, 329.1073; $C_{24}H_{12}LiN_2$, 335.1156; $C_{24}H_{12}N_2Na$, 351.0893. Anal. (%) calcd for $C_{24}H_{12}N_2$: C, 87.79; H, 3.68; N, 8.53. Found: C, 87.57; H, 3.65; N, 8.59.

Dehydro[2]pyrido[14]annulene (1c). A solution of **13c** (0.085 g, 2.59 × 10^{-4} mol) in toluene (43 mL) was added dropwise to a stirred solution of anhydrous Cu_2OAc_4 (1.880 g, 5.18 × 10^{-3} mol) in pyridine (567 mL) at 55 °C over 2.5 h. The reaction was stirred at the above temperature for a further 0.6 h, and then, the reaction worked up as described in the general macrocyclization procedure C. The aqueous KCN suspension was extracted with CH_2Cl_2 (5 × 30 mL), and the combined organic extracts were dried (anhydrous Na_2SO_4) and gravity filtered, and the solvent was removed under reduced pressure at ambient temperature. The remaining solid was then dissolved in warm CH_2Cl_2 (60 mL) and successively chromatographed three times on basic alumina (activity IV) in the absence of light, eluting with CH_2Cl_2 in all cases. The solvent was removed under vacuum from the eluate containing **1c**, at ambient temperature in darkness. The remaining solid was suspended in MeCN (5 mL), briefly ultrasonicated, isolated by filtration under vacuum, washed with MeCN (4 × 0.5 mL) and then Et_2O (3 × 0.5 mL), and air-dried at ambient temperature to constant mass to afford **1c** (0.055 g, 65%) as an off-white microcrystalline powder. ^1H NMR ($CDCl_3$, 400.13 MHz, 24 °C): δ 8.768 (dd, $^3J(6,5)$ = 4.7 Hz, $^4J(6,4)$ = 1.3 Hz, 2H; pyH6), 8.125 (m, 2H; phH3/6), 7.916 (dd, $^3J(4,5)$ = 8.0 Hz, $^4J(4,6)$ = 1.4 Hz, 2H; pyH4), 7.528 (m, 2H; phH4/5), 7.366 (dd, $^3J(5,4)$ = 7.9 Hz, $^3J(5,6)$ = 4.9 Hz, 2H; pyH5). ^{13}C NMR ($CDCl_3$, 100.61 MHz, 26 °C): δ 149.5, 147.9, 137.1, 136.6, 129.0, 122.6, 121.9, 119.9, 92.7 (−C≡), 83.7 (−C≡), 82.0 (−C≡). UV−vis (CH_2Cl_2): λ_{max} (ε) = 260 (2.6 × 10^4), 291sh (5.6 × 10^4), 299sh (6.5 × 10^4), 309 (9.2 × 10^4), 318 (6.8 × 10^4), 340sh (2.2 × 10^4), 352 (2.1 × 10^4), 366 (1.1 × 10^4), 380 nm (1.5 × 10^3 M^{-1} cm^{-1}). IR: 3075 (vw), 3040 (vw), 2192 (w) (C≡C), 2177 (w) (C≡C), 1540 (m), 1488 (m), 1435 (m), 1414 (m), 1404 (s), 1105 (m), 803 (s), 761 (s), 753 (vs), 596 (s), 517 (s), 513 cm^{-1} (s). High res. ESI MS: *m/z* (%): 327.0904 (36) [*M* + H^+], 333.0985 (13) [*M* + Li^+], 349.0720 (100) [*M* + Na^+], 365.0494 (8) [*M* + K^+], 675.1474 (54) [2*M* + Na^+], 691.1218 (8) [2*M* + K^+]. Calcd for $C_{24}H_{11}N_2$, 327.0917; $C_{24}H_{10}LiN_2$, 333.0999; $C_{24}H_{10}N_2Na$, 349.0736; $C_{24}H_{10}KN_2$, 365.0476; $C_{48}H_{20}N_4Na$, 675.1580; $C_{48}H_{20}KN_4$, 691.1320.

1,2-Bis((2-((triisopropylsilyl)ethynyl)pyridin-3-yl)ethynyl)-benzene (12d). According to general procedure A, **10d** (0.767 g, 2.71 × 10^{-3} mol), **11** (0.425 g, 1.29 × 10^{-3} mol), and $PdCl_2(PPh_3)_2$ (0.066 g, 9.40 × 10^{-5} mol) in Et_3N (20 mL), to which was added a solution of CuI (0.057 g, 2.99 × 10^{-4} mol) in Et_3N (5 mL), were stirred for 14 days and worked up to yield crude **12d**. The product was then chromatographed on a column of neutral alumina (activity III) and then rechromatographed on a column of silica, eluting with CH_2Cl_2 in both cases. Drying under vacuum at 60 °C/0.001 mm Hg and air drying yielded **12d** (0.736 g, 89%) as a pale honey-colored viscous oil. ^1H NMR ($CDCl_3$, 400.13 MHz, 24 °C): δ 8.522 (dd, $^3J(6,5)$ = 4.8 Hz, $^4J(6,4)$ = 1.5 Hz, 2H; pyH6), 7.764 (dd, $^3J(4,5)$ = 7.8 Hz, $^4J(4,6)$ = 1.6 Hz, 2H; pyH4), 7.560 (m, 2H; phH3/6), 7.351 (m, 2H; phH4/5), 7.154 (dd, $^3J(5,4)$ = 7.9 Hz, $^3J(5,6)$ = 4.8 Hz, 2H; pyH5), 1.108 (m, 42H; $CH(CH_3)_2$). ^{13}C NMR ($CDCl_3$, 100.61 MHz, 25 °C): δ 148.9, 144.3, 139.5, 131.8, 128.4, 125.6, 123.0, 122.1, 104.3 (−C≡), 96.2 (−C≡), 94.3 (−C≡), 90.0 (−C≡), 18.6 (CH-$(CH_3)_2$), 11.3 ($CH(CH_3)_2$). IR (thin film): 2942 (s), 2889 (m), 2863 (s), 1547 (m), 1455 (s), 1412 (vs), 996 (s), 881 (vs), 875 (vs), 829 (s), 796 (vs), 766 (vs), 756 (vs), 720 (s), 676 (vs), 659 (vs), 636 cm^{-1} (vs). High res. ESI MS: *m/z* (%): 641.3672 (100) [*M* + H^+], 647.3662 (6) [*M* + Li^+], 663.3450 (22) [*M* + Na^+]. Calcd for $C_{42}H_{53}N_2Si_2$, 641.3742; $C_{42}H_{52}LiN_2Si_2$, 647.3824; $C_{42}H_{52}N_2NaSi_2$, 663.3561.

1,2-Bis((2-ethynylpyridin-3-yl)ethynyl)benzene (13d). According to the general deprotection procedure B, **12d** (0.620 g, 9.67 × 10^{-4} mol) in THF (80 mL) to which 10 drops of H_2O had been added, with [(*n*-Bu)$_4$N]F (1.0 M in THF; 2.0 mL, 2.0 × 10^{-3} mol), was stirred for 1.5 days at ambient temperature. The residue that remained after removal of the solvent was partitioned between water (100 mL) and Et_2O (100 mL), and the aqueous layer was extracted with a further 60 mL of Et_2O. The combined organic extracts were further extracted with 3 × 50 mL of water, then dried (anhydrous Na_2SO_4), and gravity filtered, and the solvent was removed under reduced pressure at ambient temperature. The product was then chromatographed on a column of silica, eluting with CH_2Cl_2, to yield a honey-colored oil after removal of the solvent by distillation on a water bath and air drying. The product was boiled in heptane (240 mL) to which 0.1 g of NORIT A had been added and gravity filtered, and the filtrate was left to stand for 24 h in the dark. The crystals that formed were isolated by filtration under vacuum, washed with heptane, and air-dried. The recrystallization procedure was repeated to afford **13d** (0.217 g, 68%). ^1H NMR ($CDCl_3$, 500.13 MHz, 25 °C): δ 8.546 (dd, $^3J(6,5)$ = 4.9 Hz, $^4J(6,4)$ = 1.7 Hz, 2H; pyH6), 7.861 (dd, $^3J(4,5)$ = 8.0 Hz, $^4J(4,6)$ = 1.7 Hz, 2H; pyH4), 7.641 (m, 2H; phH3/6), 7.394 (m, 2H; phH4/5), 7.268 (dd, $^3J(5,4)$ = 8.0 Hz, $^3J(5,6)$ = 4.8 Hz, 2H; pyH5), 3.321 (s, 2H; −C≡CH). ^{13}C NMR ($CDCl_3$, 125.76 MHz, 25 °C): δ 148.9, 143.8, 139.3, 132.5, 128.8, 125.1, 123.3, 122.7, 94.5 (−C≡), 89.4 (−C≡), 81.5 (−C≡), 81.2 (−C≡). UV−vis (CH_2Cl_2): λ_{max} (ε) = 231 (5.5 × 10^4), 240sh (5.0 × 10^4), 286 (4.2 × 10^4), 306 (2.7 × 10^4), 315 (2.6 × 10^4), 326 nm; sh (2.3 × 10^4 M^{-1} cm^{-1}). IR (thin film): 3276 (s) (≡C−H), 3231 (s) (≡C−H), 3044 (w), 2106 (s) (C≡C), 1548 (s), 1484 (s), 1456 (s), 1412 (vs), 1107 (s), 1093 (s), 808 (s), 797 (vs), 767 (vs), 756 (vs), 683 (s), 669 (s), 645 cm^{-1} (vs). High res. ESI MS: *m/z* (%): 329.1040 (100) [*M* + H^+], 335.1119 (28) [*M* + Li^+], 351.0850 (33) [*M* + Na^+]. Calcd for $C_{24}H_{13}N_2$, 329.1073; $C_{24}H_{12}LiN_2$, 335.1155; $C_{24}H_{12}N_2Na$, 351.0893.

Dehydro[2]pyrido[14]annulene (1d). A solution of **13d** (0.085 g, 2.59 × 10^{-4} mol) in toluene (43 mL) was added dropwise to a stirred solution of anhydrous Cu_2OAc_4 (1.880 g, 5.18 × 10^{-3} mol) in pyridine

dx.doi.org/10.1021/jo201595s | J. Org. Chem. 2012, 77, 126–142

(567 mL) at 55 °C over 2.3 h. The reaction was stirred at the above temperature for a further 0.4 h, and then, the reaction was worked up as described in the general macrocyclization procedure C. The aqueous KCN suspension was filtered under vacuum, and the isolated solid was washed with excess water and air-dried. The filtrate was extracted with CH_2Cl_2 (2 × 100 mL), and the combined organic extracts were dried (anhydrous Na_2SO_4) and gravity filtered, and the solvent was removed under reduced pressure at ambient temperature. The residue was agitated with MeCN (5 mL), and the solvent was decanted. The remaining solid was combined with that obtained from the filtration and chromatographed on a column of basic alumina (activity IV), which was completely shielded from the light, eluting with CH_2Cl_2. The solvent was removed under vacuum from the eluate containing **1d**, at ambient temperature in darkness, to yield a solid that was suspended in MeCN (5 mL). The mixture was briefly ultrasonicated, isolated by filtration under vacuum, washed with MeCN (3 × 1 mL), and air-dried at ambient temperature to constant mass to afford **1d** (0.061 g, 72%) as a white powder. ^{1}H NMR ($CDCl_3$, 400.13 MHz, 26 °C): δ 8.687 (dd, $^3J(6,5)$ = 4.7 Hz, $^4J(6,4)$ = 1.4 Hz, 2H; pyH6), 8.163 (dd, $^3J(4,5)$ = 8.0 Hz, $^4J(4,6)$ = 1.5 Hz, 2H; pyH4), 7.936 (m, 2H; phH3/6), 7.515 (m, 2H; phH4/5), 7.431 (dd, $^3J(5,4)$ = 8.0 Hz, $^3J(5,6)$ = 4.8 Hz, 2H; pyH5). ^{13}C NMR ($CDCl_3$, 100.61 MHz, 25 °C): δ 148.9, 141.8, 139.8, 136.2, 128.6, 126.6, 122.7, 96.2 (−C≡), 90.6 (−C≡), 85.1 (−C≡), 80.2 (−C≡). UV−vis (CH_2Cl_2): λ_{max} (ε) = 299 (7.7 × 10^4), 309 (7.8 × 10^4), 318 (8.8 × 10^4), 343sh (2.1 × 10^4), 353 (1.5 × 10^4), 370 nm (1.4 × 10^4 M^{-1} cm^{-1}). IR: 3068 (w), 3034 (vw), 2182 (vw) (C≡C), 2154 (w) (C≡C), 1543 (m), 1492 (m), 1407 (m), 1106 (m), 802 (m), 754 (vs), 650 cm^{-1} (m). EI MS m/z (%): 326.1 (100) [M^+]. High res. ESI MS: m/z (%): 327.0954 (100) [M + H$^+$]. Calcd for $C_{24}H_{11}N_2$, 327.0917.

3-Bromo-2-((triisopropylsilyl)ethynyl)pyridine (15). To **14** (5.00 g, 2.11 × 10^{-2} mol) and $PdCl_2(PPh_3)_2$ (0.125 g, 1.78 × 10^{-4} mol) under argon were added consecutively by syringe N_2-purged Et_3N (80 mL) and triisopropylsilylacetylene (4.023 g, 2.21 × 10^{-2} mol), and the reaction was stirred for 0.2 h in an ice bath. A solution of CuI (0.114 g, 5.99 × 10^{-4} mol) in N_2-purged Et_3N (6 mL) was prepared in a separate Schlenk under argon and syringed into the reaction mixture. Stirring was maintained at 0−5 °C for 5 h and then at ambient temperature in the dark for 7 days. All solvent was then removed under reduced pressure on a water bath, and the residue was extracted with pentane (5 × 40 mL). The combined pentane extracts were gravity filtered, and the solvent was distilled off on a water bath at atmospheric pressure. The remaining oil was purified by distillation under vacuum to yield **15** (5.984 g, 84%) as a pale-pink oil, which distilled at 136−139 °C/0.030 mm Hg. ^{1}H NMR ($CDCl_3$, 400.13 MHz, 25 °C): δ 8.514 (dd, $^3J(6,5)$ = 4.6 Hz, $^4J(6,4)$ = 1.4 Hz, 1H; H6), 8.891 (dd, $^3J(4,5)$ = 8.2 Hz, $^4J(4,6)$ = 1.4 Hz, 1H; H4), 7.100 (dd, $^3J(5,4)$ = 8.2 Hz, $^3J(5,6)$ = 4.6 Hz, 1H; H5), 1.169 (m, 21H; CH(CH_3)$_2$). ^{13}C NMR ($CDCl_3$, 100.61 MHz, 25 °C): δ 148.0, 143.4, 139.9, 124.1, 123.6, 103.6 (−C≡), 97.8 (−C≡), 18.6 (CH(CH_3)$_2$), 11.2 (CH(CH_3)$_2$). IR (thin film): 2942 (s), 2891 (m), 2864 (s), 1564 (m), 1462 (m), 1411 (vs), 1261 (m), 1062 (s), 1019 (s), 996 (s), 882 (vs), 850 (vs), 789 (s), 752 (vs), 694 (vs), 674 (vs), 659 (vs), 629 cm^{-1} (vs). High res. ESI MS: m/z (%): 338.0948 (100) [M + H$^+$], 360.0761 (24) [M + Na$^+$]. Calcd for $C_{16}H_{25}BrNSi$, 338.0934; $C_{16}H_{24}BrNNaSi$, 360.0754.

3-Iodo-2-((triisopropylsilyl)ethynyl)pyridine (16). To a dried, argon-filled 1 L two-necked flask fitted with an alcohol thermometer, vacuum/argon inlet adaptor, and rubber septum and containing **15** (11.087 g, 3.28 × 10^{-2} mol) was added Et_2O (380 mL) via syringe. The stirred solution was cooled to −78 °C (acetone/CO_2 bath), and 1.6 M n-BuLi (23 mL, 3.68 × 10^{-2} mol) was added by syringe at a rate that maintained the internal temperature between −78 and −70 °C, and the resulting orange solution was stirred at −78 to −75 °C for 1.5 h. In a separate dried Schlenk was prepared a solution of 1,2-diiodoethane (13.00 g, 4.61 × 10^{-2} mol) in Et_2O (50 mL) under argon, and this was syringed into the lithiopyridine reaction solution at a rate that ensured that the internal temperature did not rise above −70 °C, and the reaction was stirred at −78 °C for 2 h. A solution of iodine (1.00 g, 7.88 × 10^{-3} mol) in Et_2O (10 mL) was also prepared in a dried, argon-filled Schlenk and added dropwise via syringe to the reaction at −78 °C. The reaction was stirred at −78 °C for a further 3 h and then allowed to warm to ambient temperature with continued stirring overnight. The reaction solution was extracted with dilute aqueous $Na_2S_2O_3$ (150 mL), and then water (2 × 200 mL). The combined aqueous extracts were shaken with Et_2O (150 mL), and the combined organic extracts dried (anhydrous Na_2SO_4), gravity filtered, and the solvent distilled off at atmospheric pressure on a water bath. The remaining brown oil was dried under vacuum and chromatographed on silica eluting with CH_2Cl_2. The product thus obtained was further chromatographed on three successive columns of silica, eluting with 10% Et_2O/heptane to yield **16** (11.537 g, 91%) as a faintly pale honey-colored oil after drying under vacuum. ^{1}H NMR ($CDCl_3$, 400.13 MHz, 25 °C): δ 8.541 (dd, $^3J(6,5)$ = 4.6 Hz, $^4J(6,4)$ = 1.5 Hz, 1H; H6), 8.124 (dd, $^3J(4,5)$ = 8.0 Hz, $^4J(4,6)$ = 1.5 Hz, 1H; H4), 6.935 (dd, $^3J(5,4)$ = 8.0 Hz, $^3J(5,6)$ = 4.8 Hz, 1H; H5), 1.183 (m, 21H; CH(CH_3)$_2$). ^{13}C NMR ($CDCl_3$, 100.61 MHz, 25 °C): δ 148.8, 147.4, 146.0, 123.6, 106.4, 98.7, 96.4, 18.7 (CH(CH_3)$_2$), 11.3 (CH(CH_3)$_2$). IR (thin film): 2941 (s), 2889 (m), 2863 (s), 1558 (m), 1461 (m), 1406 (vs), 1259 (m), 1062 (m), 1007 (vs), 996 (m), 882 (s), 846 (vs), 788 (s), 752 (s), 674 cm^{-1} (vs). High res. ESI MS: m/z (%): 386.0761 (100) [M + H$^+$], 408.0560 (7) [M + Na$^+$], 771.1620 (6) [2M + H$^+$]. Calcd for $C_{16}H_{25}INSi$, 386.0795; $C_{16}H_{24}INNaSi$, 408.0615; $C_{32}H_{49}I_2N_2Si_2$, 771.1518.

2-((Triisopropylsilyl)ethynyl)-3-((trimethylsilyl)ethynyl)-pyridine (17). To **16** (8.404 g, 2.18 × 10^{-2} mol) and $PdCl_2(PPh_3)_2$ (0.350 g, 4.99 × 10^{-4} mol) under argon were added N_2-purged Et_3N (150 mL) and trimethylsilylacetylene (3.684 g, 3.75 × 10^{-2} mol) consecutively by syringe. In a separate Schlenk filled with argon, a solution of CuI (0.251 g, 1.32 × 10^{-3} mol) in N_2-purged Et_3N (15 mL) was prepared and syringed into the above reaction, which resulted in an immediate color change from orange to dark gray. The mixture was stirred at ambient temperature in the dark for 9 days, and then, all solvent was removed under reduced pressure on a water bath. The residue was stirred with pentane (120 mL) and gravity filtered. The remaining solid was washed with pentane (4 × 40 mL), and the combined extracts and filtrate were stripped of solvent by distillation on a water bath at atmospheric pressure. The remaining oil was chromatographed on silica with CH_2Cl_2, and the product thus obtained was dissolved in MeCN (30 mL), briefly stirred with NORIT A (0.2 g), and gravity filtered. The filtrate was evaporated to dryness under vacuum on a water bath to afford **17** (7.575 g, 98%) as a light straw-colored oil. ^{1}H NMR ($CDCl_3$, 400.13 MHz, 25 °C): δ 8.503 (dd, $^3J(6,5)$ = 4.9 Hz, $^4J(6,4)$ = 1.7 Hz, 1H; H6), 7.756 (dd, $^3J(4,5)$ = 7.8 Hz, $^4J(4,6)$ = 1.7 Hz, 1H; H4), 7.161 (dd, $^3J(5,4)$ = 7.9 Hz, $^3J(5,6)$ = 4.9 Hz, 1H; H5), 1.173 (m, 21H; CH(CH_3)$_2$), 0.250 (s, 9H; Si(CH_3)$_3$).

1,3-Bis((4-((triisopropylsilyl)ethynyl)pyridin-3-yl)ethynyl)-benzene (19a). According to the general procedure A, **10a** (0.600 g, 2.12 × 10^{-3} mol), **18** (0.350 g, 1.06 × 10^{-3} mol), and $PdCl_2(PPh_3)_2$ (0.100 g, 1.42 × 10^{-4} mol) in Et_3N (30 mL), to which was added a solution of CuI (0.100 g, 5.25 × 10^{-4} mol) in Et_3N (6 mL), was stirred for 15 days and worked up to yield crude **19a**. The product was then chromatographed on three successive columns of neutral alumina (activity III), with CH_2Cl_2 as the eluant. Removal of the solvent by distillation on a water bath at atmospheric pressure, drying under vacuum at 60 °C/0.001 mm Hg, and air drying yielded **19a** (0.490 g, 72%) as a pale honey-colored viscous oil. ^{1}H NMR ($CDCl_3$, 400.13 MHz, 25 °C): δ 8.750 (s, 2H; pyH2), 8.481 (d, $^3J(6,5)$ = 5.1 Hz, 2H; pyH6), 7.755 (td, $^4J(2,4/2,6)$ = 1.4 Hz, $^5J(2,5)$ = 0.5 Hz, 1H; phH2), 7.519 (dd, $^3J(4,5/6,5)$ = 7.8 Hz, $^4J(4,2/6,2)$ = 1.6 Hz, 2H; phH4/6), 7.364 (dd, $^3J(5,6)$ = 5.1 Hz, $^5J(5,2)$ = 0.7 Hz, 2H; pyH5), 7.353 (td, $^3J(5,4/5,6)$ = 7.6 Hz, $^5J(5,2)$ = 0.6 Hz, 1H; phH5), 1.128 (m, 42H; CH(CH_3)$_2$). ^{13}C NMR ($CDCl_3$, 100.61 MHz, 26 °C): δ 152.6, 148.1, 135.2, 133.2, 131.8, 128.4, 125.8, 123.0, 121.7, 102.5 (−C≡), 101.5 (−C≡), 94.8 (−C≡), 85.9 (−C≡), 18.6 (CH(CH_3)$_2$), 11.2 (CH(CH_3)$_2$). IR (thin film): 2941 (s), 2891 (m), 2864 (s), 1572 (s), 1485 (s), 1462 (s), 1399 (s), 996 (m), 882 (vs), 863 (vs), 842 (vs), 832 (vs), 794 (vs), 679 (vs), 663 (vs), 641 cm^{-1} (vs). High res. ESI MS: m/z (%): 641.3666 (100) [M + H$^+$]. Calcd for $C_{42}H_{53}N_2Si_2$, 641.3742.

dx.doi.org/10.1021/jo201595s | J. Org. Chem. 2012, 77, 126−142

1,3-Bis((4-ethynylpyridin-3-yl)ethynyl)benzene (20a). According to the general deprotection procedure B, **19a** (0.430 g, 6.71×10^{-4} mol) in THF (25 mL) to which H_2O (1 mL) had been added, with $[(n\text{-Bu})_4N]F$ (1.0 M in THF; 2.2 mL, 2.2×10^{-3} mol), was stirred at ambient temperature for 3 days. The residue that remained after removal of the solvent was partitioned between water (150 mL) and CH_2Cl_2 (150 mL) and extracted further with CH_2Cl_2 (2×150 mL). The combined organic extracts were extracted with water (100 mL), dried (anhydrous $MgSO_4$), gravity filtered, and concentrated to 20 mL by distillation on a water bath. The concentrate was chromatographed on neutral alumina (activity III), eluting with CH_2Cl_2, and the product thus isolated was recrystallized from heptane as described for the purification of **13d** above to afford **20a** (0.105 g, 48%) as a crystalline cream solid after air drying. ^{1}H NMR ($CDCl_3$, 400.13 MHz, 23 °C): δ 8.784 (s, 2H; pyH2), 8.518 (d, $^3J(6,5) = 5.1$ Hz, 2H; pyH6), 7.777 (t, $^4J(2,4/2,6) = 1.5$ Hz, 1H; phH2), 7.578 (dd, $^3J(4,5/6,5) = 7.8$ Hz, $^4J(4,2/6,2) = 1.4$ Hz, 2H; phH4/6), 7.393 (m, 3H; phH5/pyH5), 3.596 (s, 2H; −C≡CH). ^{13}C NMR ($CDCl_3$, 100.61 MHz, 26 °C): δ 152.4, 148.3, 134.9, 132.2, 132.1, 128.7, 125.7, 123.0, 122.1, 95.3 (−C≡), 85.8 (−C≡), 85.5 (−C≡), 79.7 (−C≡). UV−vis (CH_2Cl_2): λ_{max} (ε) = 242 (5.6×10^4), 280sh (3.4×10^4), 287sh (3.7×10^4), 295 (4.2×10^4), 316 (3.4×10^4), 325 nm (3.4×10^4 M^{-1} cm^{-1}). IR (thin film): 3121 (s) (≡C−H), 2219 (w) (C≡C), 2097 (s) (C≡C), 1579 (s), 1567 (s), 1478 (s), 1399 (s), 1050 (s), 896 (s), 829 (vs), 795 (vs), 754 (vs), 731 (s), 683 cm^{-1} (vs). High res. ESI MS: m/z (%): 329.1070 (100) [M + H^+], 351.0911 (11) [M + Na^+]. Calcd for $C_{24}H_{13}N_2$, 329.1073; $C_{24}H_{12}N_2Na$, 351.0893.

Dehydro[2]pyrido[15]annulene (2a). A solution of **20a** (0.060 g, 1.83×10^{-4} mol) in toluene (30 mL) was added dropwise to a stirred solution of anhydrous Cu_2OAc_4 (1.330 g, 3.66×10^{-3} mol) in pyridine (400 mL) at 55 °C over 2 h. The reaction was stirred at the above temperature for a further 1 h, and then, the reaction worked up as described in the general macrocyclization procedure C. The aqueous KCN suspension was extracted with CH_2Cl_2 (3×250 mL), and the combined organic extracts were dried (anhydrous Na_2SO_4) and gravity filtered, and the solvent removed under vacuum at ambient temperature. The remaining solid was stirred in hot CH_2Cl_2 (60 mL) and twice chromatographed on neutral alumina (activity III) with CH_2Cl_2 as the eluant. The product thus obtained was suspended in ice-cold CH_2Cl_2 (6 mL), briefly ultrasonicated, isolated by filtration under vacuum, washed with ice-cold CH_2Cl_2 (3×1 mL), and air-dried at ambient temperature to constant mass to afford **2a** (0.033 g, 55%) as a pale yellow solid. ^{1}H NMR ($CDCl_3$, 400.13 MHz, 25 °C): δ 8.701 (d, $^5J(2,5) = 0.7$ Hz, 2H; pyH2), 8.652 (m, 1H; phH2), 8.549 (d, $^3J(6,5) = 5.1$ Hz, 2H; pyH6), 7.400 (dd, $^3J(5,6) = 5.1$ Hz, $^5J(5,2) = 0.8$ Hz, 2H; pyH5), 7.368 (m, 3H; phH4/6, phH5). ^{13}C NMR ($CDCl_3$, 100.61 MHz, 26 °C): δ 150.4, 148.5, 145.4, 133.1, 129.0, 127.9, 125.5, 123.4, 123.1, 99.5 (−C≡), 89.1 (−C≡), 81.4 (−C≡), 81.2 (−C≡). UV−vis (CH_2Cl_2): λ_{max} (ε) = 284 (9.3×10^4), 303sh (5.4×10^4), 331 (2.1×10^4), 353 (9.0×10^3), 376 (3.9×10^3), 401 nm (2.0×10^3 M^{-1} cm^{-1}). IR: 3045 (vw), 3009 (vw), 2199 (m) (C≡C), 1569 (s), 1520 (m), 1482 (m), 1409 (s), 1395 (m), 1264 (m), 892 (m), 830 (vs), 803 (s), 789 (vs), 746 (m), 726 (m), 676 cm^{-1} (s). EI MS m/z (%): 326.1 (100) [M^+]. High res. ESI MS: m/z (%): 327.0873 (100) [M + H^+]. Calcd for $C_{24}H_{11}N_2$, 327.0917.

1,3-Bis((3-((triisopropylsilyl)ethynyl)pyridin-4-yl)ethynyl)-benzene (19b). According to general procedure A, **10b** (0.600 g, 2.12×10^{-3} mol), **18** (0.350 g, 1.06×10^{-3} mol), and $PdCl_2(PPh_3)_2$ (0.140 g, 1.99×10^{-4} mol) in Et_3N (30 mL), to which was added a solution of CuI (0.140 g, 7.40×10^{-4} mol) in Et_3N (6 mL), were stirred for 21 days and worked up to yield crude **19b**. The product was then chromatographed on silica, first with CH_2Cl_2 as the eluant, and then, the solvent polarity was increased from 0.5−1% $MeOH/CH_2Cl_2$ to elute the **19b**. Removal of the solvent by distillation on a water bath at atmospheric pressure, drying under vacuum at 60 °C/0.001 mm Hg, and air drying yielded **19b** (0.316 g, 46%) as a pale honey-colored viscous oil. ^{1}H NMR ($CDCl_3$, 400.13 MHz, 25 °C): δ 8.742 (s, 2H; pyH2), 8.503 (d, $^3J(6,5) = 5.1$ Hz, 2H; pyH6), 7.762 (t, $^4J(2,4/2,6) = 1.4$ Hz, 1H; phH2), 7.547 (dd, $^3J(4,5/6,5) = 7.7$ Hz, $^4J(4,2/6,2) = 1.7$ Hz, 2H; phH4/6), 7.375 (t, $^3J(5,4/5,6) = 7.7$ Hz, 1H; phH5), 7.360 (d, $^3J(5,6) = 5.0$ Hz, 2H; pyH5), 1.132 (m, 42H; $CH(CH_3)_2$). ^{13}C NMR ($CDCl_3$, 100.61 MHz, 24 °C): δ 153.3, 148.0, 135.4, 132.9, 132.3, 128.5, 125.0, 122.7, 122.0, 102.0 (−C≡), 99.1 (−C≡), 96.2 (−C≡), 86.6 (−C≡), 18.6 ($CH(CH_3)_2$), 11.3 ($CH(CH_3)_2$). IR (thin film): 2942 (s), 2891 (m), 2863 (s), 2218 (m) (C≡C), 2159 (m) (C≡C), 1574 (s), 1488 (s), 1462 (s), 1413 (m), 1399 (m), 1190 (m), 994 (s), 882 (vs), 862 (m), 839 (m), 826 (vs), 797 (vs), 730 (m), 680 (vs), 669 (vs), 656 (vs) cm^{-1}. High res. ESI MS: m/z (%): 641.3727 (100) [M + H^+]. Calcd for $C_{42}H_{53}N_2Si_2$, 641.3742.

1,3-Bis((3-ethynylpyridin-4-yl)ethynyl)benzene (20b). According to the general deprotection procedure B, **19b** (0.270 g, 4.21×10^{-4} mol) in THF (25 mL) to which H_2O (1 mL) had been added, with $[(n\text{-Bu})_4N]F$ (1.0 M in THF; 1.4 mL, 1.4×10^{-3} mol), was stirred at ambient temperature for 3 days. The residue that remained after removal of the solvent was partitioned between water (150 mL) and CH_2Cl_2 (150 mL) and extracted further with CH_2Cl_2 (2×150 mL). The combined organic extracts were extracted with water (100 mL), dried (anhydrous Na_2SO_4), gravity filtered, and concentrated to 20 mL by distillation on a water bath. The concentrate was chromatographed on neutral alumina (activity III), eluting with CH_2Cl_2, and the product thus isolated was recrystallized from heptane as described for the purification of **13d** above to afford **20b** (0.107 g, 77%) as a crystalline cream solid after air drying. ^{1}H NMR ($CDCl_3$, 400.13 MHz, 27 °C): δ 8.768 (d, $^5J(2,5) = 0.7$ Hz, 2H; pyH2), 8.554 (d, $^3J(6,5) = 5.3$ Hz, 2H; pyH6), 7.795 (t, $^4J(2,4/2,6) = 1.5$ Hz, 1H; phH2), 7.613 (dd, $^3J(4,5/6,5) = 7.8$ Hz, $^4J(4,2/6,2) = 1.6$ Hz, 2H; phH4/6), 7.421 (t, $^3J(5,4/5,6) = 8.0$ Hz, 1H; phH5), 7.393 (dd, $^3J(5,6) = 5.2$ Hz, $^5J(5,2) = 0.8$ Hz, 2H; pyH5), 3.499 (s, 2H; −C≡CH). ^{13}C NMR ($CDCl_3$, 100.61 MHz, 25 °C): δ 153.2, 148.7, 135.3, 133.4, 132.8, 128.8, 124.9, 122.6, 120.7, 96.7 (−C≡), 86.2 (−C≡), 84.2 (−C≡), 79.2 (−C≡). UV−vis (CH_2Cl_2): λ_{max} (ε) = 228 (4.1×10^4), 246 (4.7×10^4), 300 (4.7×10^4), 313 nm; sh (4.0×10^4 M^{-1} cm^{-1}). IR (thin film): 3219 (m) (≡C−H), 3148 (m) (≡C−H), 3032 (w), 2215 (m) (C≡C), 2097 (m) (C≡C), 1593 (m), 1578 (s), 1528 (m), 1487 (m), 1404 (m), 1399 (m), 1188 (m), 1049 (m), 943 (s), 904 (s), 836 (vs), 795 (vs), 704 (s), 681 cm^{-1} (vs). High res. ESI MS: m/z (%): 329.1065 (100) [M + H^+]. Calcd for $C_{24}H_{13}N_2$, 329.1073.

Dehydro[2]pyrido[15]annulene (2b). A solution of **20b** (0.075 g, 2.28×10^{-4} mol) in toluene (30 mL) was added dropwise to a stirred solution of anhydrous Cu_2OAc_4 (1.680 g, 4.62×10^{-3} mol) in pyridine (500 mL) at 55 °C over 1.25 h. The reaction was stirred at the above temperature for a further 0.25 h and worked up as described in the general macrocyclization procedure C. The aqueous KCN suspension was filtered under vacuum, and the isolated solid was washed with excess distilled water and air-dried. The crude product was then stirred with warm CH_2Cl_2 (30 mL) and chromatographed in the dark on silica with CH_2Cl_2 as the eluant. The solid thus isolated was washed successively with Et_2O and MeCN, air-dried, and rechromatographed on silica with CH_2Cl_2. The product was then chromatographed on a short column of basic alumina (activity III) completely shielded from the light, eluting with CH_2Cl_2. All solvent was removed from the eluate containing **2b** under vacuum at ambient temperature in darkness. The remaining solid was suspended in MeCN (5 mL), briefly ultrasonicated, isolated by filtration under vacuum, washed with MeCN (4×0.5 mL) and then Et_2O (3×0.5 mL), and air-dried at ambient temperature to constant mass to afford **2b** (0.043 g, 58%) as an amorphous white powder. The product can be recrystallized from MeCN. ^{1}H NMR ($CDCl_3$, 400.13 MHz, 27 °C): δ 8.758 (s, 2H; pyH2), 8.731 (s, 1H; phH2), 8.557 (d, $^3J(6,5) = 5.1$ Hz, 2H; pyH6), 7.406 (m, 3H; phH4/6, phH5), 7.282 (d, $^3J(5,6) = 5.3$ Hz, 2H; pyH5). ^{13}C NMR ($CDCl_3$, 100.61 MHz, 23 °C): δ 152.6, 149.2, 146.2, 134.8, 129.1, 129.0, 123.1, 122.8, 122.2, 100.5 (−C≡), 89.9 (−C≡), 80.9 (−C≡), 80.5 (−C≡). UV−vis (CH_2Cl_2): λ_{max} (ε) = 292 (1.1×10^5), 326sh (2.9×10^4), 339 (2.0×10^4), 363 (1.0×10^4), 374 (9.3×10^3), 393 nm (9.3×10^3 M^{-1} cm^{-1}). IR: 3050 (m), 3014 (m), 2199 (s) (C≡C), 2159 (m) (C≡C), 1582 (vs), 1573 (vs), 1520 (m), 1487 (s), 1411 (s), 1396 (s), 1262 (m), 1186 (m), 898 (s), 828 (s), 785 (s), 747 (m), 679 (s), 672 (m), 576 cm^{-1} (s). EI MS m/z (%): 326.0 (100) [M^+]. High res. ESI MS: m/z (%): 327.0909 (100) [M + H^+], 333.1003 (19) [M + Li^+], 349.0806 (9) [M + Na^+].

dx.doi.org/10.1021/jo201595s | J. Org. Chem. 2012, 77, 126−142

Calcd for $C_{24}H_{11}N_2$, 327.0917; $C_{24}H_{10}LiN_2$, 333.0999; $C_{24}H_{10}N_2Na$, 349.0736.

2,6-Bis((4-((triisopropylsilyl)ethynyl)pyridin-3-yl)ethynyl)-pyridine (22). According to general procedure A, **10a** (0.700 g, 2.47×10^{-3} mol), **21** (0.290 g, 1.22×10^{-3} mol), and $PdCl_2(PPh_3)_2$ (0.064 g, 9.12×10^{-5} mol) in Et_3N (25 mL), to which was added a solution of CuI (0.063 g, 3.31×10^{-4} mol) in Et_3N (7 mL), were stirred for 21 days. After the solvent was removed, the residue was extracted with hot heptane (5 × 30 mL), the combined extracts were gravity filtered, and the solvent was removed under reduced pressure on a water bath to yield crude **22**. The product was then twice chromatographed on basic alumina (activity IV) and then on a short column of neutral alumina (activity III) with CH_2Cl_2 as the eluant. Removal of the solvent by distillation on a water bath at atmospheric pressure, drying under vacuum at 60 °C/0.001 mm Hg, and air drying yielded **22** (0.608 g, 77%) as a pale honey-colored vitreous semisolid. ^{1}H NMR ($CDCl_3$, 400.13 MHz, 25 °C): δ 8.821 (d, ^5J(2,5) = 0.5 Hz, 2H; terminal pyH2), 8.514 (d, ^3J(6,5) = 5.1 Hz, 2H; terminal pyH6), 7.688 (t, ^3J(4,3/4,5) = 7.9 Hz, 1H; central pyH4), 7.490 (d, ^3J(3,4/5,4) = 7.9 Hz, 2H; central pyH3/5), 7.370 (dd, ^3J(5,6) = 5.1 Hz, ^5J(5,2) = 0.7 Hz, 2H; terminal pyH5), 1.127 (m, 42H; $CH(CH_3)_2$). ^{13}C NMR ($CDCl_3$, 100.61 MHz, 25 °C): δ 153.0, 148.7, 143.3, 136.1, 133.5, 126.7, 125.7, 120.9, 102.3 (−C≡), 101.9 (−C≡), 94.2 (−C≡), 85.2 (−C≡), 18.6 ($CH(CH_3)_2$), 11.2 ($CH(CH_3)_2$). IR (thin film): 2941 (s), 2889 (m), 2863 (s), 1571 (s), 1556 (s), 1479 (s), 1462 (m), 1441 (vs), 1399 (m), 1158 (m), 996 (m), 881 (s), 864 (s), 842 (vs), 806 (s), 797 (s), 752 (m), 677 (vs), 663 (vs), 641 cm^{-1} (s). High res. ESI MS: m/z (%): 642.3621 (100) [M + H$^+$], 648.3700 (79) [M + Li$^+$], 664.3437 (4) [M + Na$^+$]. Calcd for $C_{41}H_{52}N_3Si_2$, 642.3694; $C_{41}H_{51}LiN_3Si_2$, 648.3777; $C_{41}H_{51}N_3NaSi_2$, 664.3514.

2,6-Bis((4-ethynylpyridin-3-yl)ethynyl)pyridine (23). According to the general deprotection procedure B, **22** (0.570 g, 8.88×10^{-4} mol) in THF (40 mL) to which 6 drops of H_2O had been added, with [(n-Bu)$_4$N]F (1.0 M in THF; 1.8 mL, 1.8×10^{-3} mol), was stirred at ambient temperature for 1 day. The residue that remained after removal of the solvent was shaken with Et_2O (2 × 80 mL), and the extracts were decanted off. Distilled water (60 mL) was then added to the residue, and the suspended solid was isolated by filtration under vacuum, washed with excess water, and air-dried. The Et_2O extracts were shaken with water (100 mL), dried (anhydrous Na_2SO_4), and gravity filtered, and the solvent was removed by distillation on a water bath. Pentane (60 mL) was then added to the remaining oil, which caused precipitation of a solid, after which the pentane was decanted off. All isolated solids were combined and chromatographed on basic alumina (activity IV) eluting with CH_2Cl_2. The product isolated from the chromatography was dissolved in boiling methylcyclohexane (300 mL) and gravity filtered, and all solvent removed under reduced pressure on a water bath. Decolorizing carbon (NORIT A) and CH_2Cl_2 (10 mL) were added to the product, and the mixture briefly stirred and gravity filtered, and all solvent removed from the filtrate by distillation under reduced pressure at ambient temperature. The product was then suspended in MeCN (5 mL), briefly ultrasonicated, filtered under vacuum, and washed with MeCN (3 × 1 mL) to afford **23** (0.161 g, 55%) as a microcrystalline cream powder after air drying. ^{1}H NMR ($CDCl_3$, 400.13 MHz, 26 °C): δ 8.855 (d, ^5J(2,5) = 0.5 Hz, 2H; terminal pyH2), 8.558 (d, ^3J(6,5) = 5.3 Hz, 2H; pyH6), 7.745 (t, ^3J(4,3/4,5) = 7.8 Hz, 1H; central pyH4), 7.576 (d, ^3J(3,4/5,4) = 7.7 Hz, 2H; central pyH3/5), 7.412 (d, ^3J(5,6) = 5.1 Hz, 2H; terminal pyH5), 3.612 (s, 2H; −C≡CH). ^{13}C NMR ($CDCl_3$, 100.61 MHz, 26 °C): δ 152.9, 148.9, 143.3, 136.6, 132.6, 127.3, 125.8, 121.2, 94.5 (−C≡), 86.3 (−C≡), 84.9 (−C≡), 79.5 (−C≡). UV−vis (CH_2Cl_2): λ_{max} (ε) = 228 (4.3×10^4), 238 (4.4×10^4), 278 (2.3×10^4), 321 (2.9×10^4), 330 nm (3.1×10^4 M^{-1} cm^{-1}). IR (thin film): 3301 (m) (≡C−H), 3189 (m) (≡C−H), 3008 (w), 2102 (m) (C≡C), 1570 (s), 1557 (s), 1476 (m), 1440 (s), 1396 (m), 1206 (m), 983 (m), 845 (s), 827 (s), 804 (s), 758 (m), 752 (s), 726 (s), 654 (s), 617 cm^{-1} (s). High res. ESI MS: m/z (%): 330.1007 (100) [M + H$^+$], 659.1911 (7) [2M + H$^+$]. Calcd for $C_{23}H_{12}N_3$, 330.1026; $C_{46}H_{23}N_6$, 659.1979.

Dehydro[3]pyrido[15]annulene (3). A solution of **23** (0.067 g, 2.03×10^{-4} mol) in toluene (30 mL) was added dropwise to a stirred solution of anhydrous Cu_2OAc_4 (1.880 g, 5.18×10^{-3} mol) in pyridine (567 mL) at 55 °C over 0.7 h. The reaction was stirred at the above temperature for a further 0.25 h and worked up as described in the general macrocyclization procedure C. The aqueous KCN suspension was filtered under vacuum, and the isolated dark brown/black solid was washed with excess distilled water and air-dried. The aqueous filtrate was extracted with CH_2Cl_2 (4 × 60 mL). The solid was ultrasonicated with hot CH_2Cl_2 (100 mL) and filtered under gravity. The CH_2Cl_2 extracts and filtrate were combined, and the solvent was removed under reduced pressure at ambient temperature. The remaining grayish-colored solid was dissolved in CH_2Cl_2 (25 mL) and chromatographed in the dark on basic alumina (activity IV) with CH_2Cl_2 as the eluant. All solvent was removed from the eluate containing **3** under vacuum at ambient temperature in darkness. The remaining solid was suspended in MeCN (5 mL), briefly ultrasonicated, isolated by filtration under vacuum, washed with MeCN (4 × 0.5 mL) and then Et_2O (3 × 0.5 mL), and air-dried at ambient temperature to constant mass to afford **3** (0.024 g, 36%) as a lemon-yellow micofibrous solid. ^{1}H NMR ($CDCl_3$, 400.13 MHz, 26 °C): δ 8.688 (s, 2H; terminal pyH2), 8.556 (d, ^3J(6,5) = 5.1 Hz, 2H; terminal pyH6), 7.679 (t, ^3J(4,3/4,5) = 7.8 Hz, 1H; central pyH4), 7.371 (d, ^3J(5,6) = 5.1 Hz, 2H; terminal pyH5), 7.311 (d, ^3J(3,4/5,4) = 7.8 Hz, 2H; central pyH3/5). ^{13}C NMR ($CDCl_3$, 100.61 MHz, 26 °C): δ 150.5, 149.2, 144.0, 137.3, 134.8, 125.5, 123.5, 122.7, 99.1 (−C≡), 86.7 (−C≡), 82.9 (−C≡), 80.1 (−C≡). UV−vis (CH_2Cl_2): λ_{max} (ε) = 275 (6.4×10^4), 293 (6.1×10^4), 307 (8.3×10^4), 324sh (2.1×10^4), 338 (2.1×10^4), 377 (3.2×10^3), 405 nm (1.2×10^3 M^{-1} cm^{-1}). IR: 3051 (w), 3008 (vw), 2160 (w) (C≡C), 2139 (w) (C≡C), 1586 (m), 1573 (s), 1552 (m), 1474 (s), 1447 (m), 1411 (s), 1269 (m), 1152 (m), 980 (m), 833 (s), 827 (s), 802 (vs), 747 (m), 729 (m), 579 (s), 557 cm^{-1} (s). EI MS m/z (%): 327.1 (100) [M^+]. High res. ESI MS: m/z (%): 328.0845 (62) [M + H$^+$], 334.0927 (66) [M + Li$^+$], 350.0661 (100) [M + Na$^+$], 677.1476 (18) [2M + Na$^+$]. Calcd for $C_{23}H_{10}N_3$, 328.0869; $C_{23}H_9LiN_3$, 334.0951; $C_{23}H_9N_3Na$, 350.0689; $C_{46}H_{18}N_6Na$, 677.1485.

■ ASSOCIATED CONTENT

Ⓢ Supporting Information

Synthesis of dehydro[m]pyrido[14]- and [15]annulenes **1a−d**, **2a,b**, and **3**; general experimental; spectroscopic characterization of macrocycles **1a−d**, **2a,b**, and **3** and precursors **12a−d** and **13a−d**; ^{1}H NMR investigation of solution aggregation of **1a**; ^{1}H and ^{13}C NMR solution spectra of **1a−d**, **2a,b**, **3**, **12a−d**, **13a−d**, **15−17**, **19a,b**, **20a,b**, **22**, and **23**; UV−vis spectroscopic properties of precursors **13a−d**, **20a,b**, and **23** and UV−vis absorption spectra of **1a−d**, **2a,b**, and **3** with $Hg(CF_3SO_3)_2$; general X-ray experimental, crystallographic data, and ORTEP representations for **1b** and **1c**; HOMO and LUMO plots of **1c,d** and **2b**; linear regression through origin of optical bandgap *vs* calculated bandgap for **1a−1d**, **2a,b**, and **3**; calculated structure Cartesian coordinates of **1a−d**, **2a,b**, and **3**; and references (continued). This material is available free of charge via the Internet at http://pubs.acs.org.

■ AUTHOR INFORMATION

Corresponding Author

*E-mail: paul.baxter@ics-cnrs.unistra.fr.

■ ACKNOWLEDGMENTS

The Centre National de la Recherche Scientifique and the Institut Charles Sadron are acknowledged for financial support (P.N.W.B.), along with the Ministère de l'Enseignement Supérieur et de la Recherche for a Ph.D. fellowship (A.A.). Dr. Raymonde Baltenweck-Guyot and Romain Carriere of the Service de Spectrometrie de Masse, Inst. de Chimie, UdS, are

thanked for the MALDI and ESI mass spectrometric measurements. Dr. Roland Graff and Dr. Lionel Allouche of the Service de RMN, Inst. de Chimie, UdS, are thanked for the NOESY, ROESY, HMQC, HSQC, and DOSY NMR measurements, and Y. Guilbert of the ICS is thanked for the TGA measurements. Jacques Druz and Marie-France Peguet of the Service de Microanalyse, ICS, are thanked for the elemental analyses, and Pascal Disdier (MISHA, CNRS, UdS) is thanked for the photographic images.

REFERENCES

(1) Marsden, J. A.; Palmer, G. J.; Haley, M. M. *Eur. J. Org. Chem.* **2003**, 2355−2369. The term "dehydroaryl[*n*]annulene" is used in the context of this work specifically for macrocycles comprising a purely unsaturated organic (carbon-based) covalent framework, with predominantly *ortho*-connectivity at the aromatic rings.
(2) Kennedy, R. D.; Lloyd, D.; McNab, H. *J. Chem. Soc., Perkin Trans. 1*, **2002**, 1601−1621.
(3) Haley, M. M.; Pak, J. J.; Brand, S. C. In *Carbon Rich Compounds II*; de Meijere, A., Ed.; Top. Curr. Chem., Vol. 201; Springer: Berlin, 1999, pp 81−130.
(4) Youngs, W. J.; Tessier, C. A.; Bradshaw, J. D. *Chem. Rev.* **1999**, *99*, 3153−3180.
(5) Haley, M. M. *Synlett* **1998**, 557−565.
(6) Mitchell, R. H. *Isr. J. Chem.* **1980**, *20*, 294−299.
(7) Meier, H. *Synthesis* **1972**, 235−253.
(8) Tahara, K.; Yoshimura, T.; Sonoda, M.; Tobe, Y.; Williams, R. V. *J. Org. Chem.* **2007**, *72*, 1437−1442.
(9) Narita, N.; Nagai, S.; Suzuki, S. *Phys. Rev. B* **2001**, *64*, 245408-1−245408-7.
(10) Narita, N.; Nagai, S.; Suzuki, S.; Nakao, K. *Phys. Rev. B* **2000**, *62*, 11146−11151.
(11) Bunz, U. H. F.; Rubin, Y.; Tobe, Y. *Chem. Soc. Rev.* **1999**, *28*, 107−119.
(12) Narita, N.; Nagai, S.; Suzuki, S.; Nakao, K. *Phys. Rev. B* **1998**, *58*, 11009−11014.
(13) Diederich, F. *Nature* **1994**, *369*, 199−207.
(14) Diederich, F.; Rubin, Y. *Angew. Chem., Int. Ed. Engl.* **1992**, *31*, 1101−1123.
(15) Baughman, R. H.; Eckhardt, H.; Kertesz, M. *J. Chem. Phys.* **1987**, *87*, 6687−6699.
(16) Yoshimura, T.; Inaba, A.; Sonoda, M.; Tahara, K.; Tobe, Y.; Williams, R. V. *Org. Lett.* **2006**, *8*, 2933−2936.
(17) Marsden, J. A.; Haley, M. M. *J. Org. Chem.* **2005**, *70*, 10213−10226.
(18) Sonoda, M.; Sakai, Y.; Yoshimura, T.; Tobe, Y.; Kamada, K. *Chem. Lett.* **2004**, *33*, 972−973.
(19) Iyoda, M.; Sirinintasak, S.; Nishiyama, Y.; Vorasingha, A.; Sultana, F.; Nakao, K.; Kuwatani, Y.; Matsuyama, H.; Yoshida, M.; Miyake, Y. *Synthesis* **2004**, 1527−1531.
(20) Miljanić, O. Š.; Vollhardt, K. P. C.; Whitener, G. D. *Synlett* **2003**, 29−34.
(21) Kehoe, J. M.; Kiley, J. H.; English, J. J.; Johnson, C. A.; Petersen, R. C.; Haley, M. M. *Org. Lett.* **2000**, *2*, 969−972.
(22) Wan, W. B.; Brand, S. C.; Pak, J. J.; Haley, M. M. *Chem.—Eur. J.* **2000**, *6*, 2044−2052.
(23) Bhaskar, A.; Guda, R.; Haley, M. M.; Goodson, T. III. *J. Am. Chem. Soc.* **2006**, *128*, 13972−13973.
(24) Zhou, X.; Ren, A.-M.; Feng, J.-K.; Liu, X.-J. *Can. J. Chem.* **2004**, *82*, 1172−1178.
(25) Sarkar, A.; Pak, J. J.; Rayfield, G. W.; Haley, M. M. *J. Mater. Chem.* **2001**, *11*, 2943−2945.
(26) Kimball, D. B.; Haley, M. M.; Mitchell, R. H.; Ward, T. R.; Bandyopadhyay, S.; Williams, R. V.; Armantrout, J. R. *J. Org. Chem.* **2002**, *67*, 8798−8811.
(27) Kimball, D. B.; Haley, M. M.; Mitchell, R. H.; Ward, T. R. *Org. Lett.* **2001**, *3*, 1709−1711.
(28) Nishide, H.; Takahashi, M.; Takashima, J.; Pu, Y.-J.; Tsuchida, E. *J. Org. Chem.* **1999**, *64*, 7375−7380.
(29) Pu, Y. J.; Takahashi, M.; Tsuchida, E.; Nishide, H. *Chem. Lett.* **1999**, 161−162.
(30) Staab, H. A.; Graf, F. *Chem. Ber.* **1970**, *103*, 1107−1118.
(31) Seo, S. H.; Jones, T. V.; Seyler, H.; Peters, J. O.; Kim, T. H.; Chang, J. Y.; Tew, G. N. *J. Am. Chem. Soc.* **2006**, *128*, 9264−9265.
(32) Collins, S. K.; Yap, G. P. A.; Fallis, A. G. *Org. Lett.* **2000**, *2*, 3189−3192.
(33) Ferrara, J. D.; Tanaka, A. A.; Fierro, C.; Tessier-Youngs, C. A.; Youngs, W. J. *Organometallics* **1989**, *8*, 2089−2098.
(34) Laskoski, M.; Steffen, W.; Morton, J. G. M.; Smith, M. D.; Bunz, U. H. F. *J. Am. Chem. Soc.* **2002**, *124*, 13814−13818.
(35) Glezakou, V.-A.; Boatz, J. A.; Gordon, M. S. *J. Am. Chem. Soc.* **2002**, *124*, 6144−6152.
(36) Dosa, P. I.; Erben, C.; Iyer, V. S.; Vollhardt, K. P. C.; Wasser, I. M. *J. Am. Chem. Soc.* **1999**, *121*, 10430−10431.
(37) Boese, R.; Matzger, A. J.; Vollhardt, K. P. C. *J. Am. Chem. Soc.* **1997**, *119*, 2052−2053.
(38) Spitler, E. L.; Monson, J. M.; Haley, M. M. *J. Org. Chem.* **2008**, *73*, 2211−2223.
(39) Hisaki, I.; Sonoda, M.; Tobe, Y. *Eur. J. Org. Chem.* **2006**, 833−847.
(40) Marsden, J. A.; Miller, J. J.; Shirtcliff, L. D.; Haley, M. M. *J. Am. Chem. Soc.* **2005**, *127*, 2464−2476.
(41) Hisaki, I.; Eda, T.; Sonoda, M.; Niino, H.; Sato, T.; Wakabayashi, T.; Tobe, Y. *J. Org. Chem.* **2005**, *70*, 1853−1864.
(42) Marsden, J. A.; Miller, J. J.; Haley, M. M. *Angew. Chem., Int. Ed.* **2004**, *43*, 1694−1697.
(43) Tobe, Y.; Ohki, I.; Sonoda, M.; Niino, H.; Sato, T.; Wakabayashi, T. *J. Am. Chem. Soc.* **2003**, *125*, 5614−5615.
(44) Tobe, Y.; Kishi, J.; Ohki, I.; Sonoda, M. *J. Org. Chem.* **2003**, *68*, 3330−3332.
(45) Boydston, A. J.; Laskoski, M.; Bunz, U. H. F.; Haley, M. M. *Synlett* **2002**, 981−983.
(46) Baldwin, K. P.; Matzger, A. J.; Scheiman, D. A.; Tessier, C. A.; Vollhardt, K. P. C.; Youngs, W. J. *Synlett* **1995**, 1215−1218.
(47) Zhou, Q.; Carroll, P. J.; Swager, T. M. *J. Org. Chem.* **1994**, *59*, 1294−1301.
(48) Pak., J. J.; Weakley, T. J. R.; Haley, M. M.; Lau, D. Y. K.; Stoddart, J. F. *Synthesis* **2002**, 1256−1260.
(49) Furukawa, S.; Uji-i, H.; Tahara, K.; Ichikawa, T.; Sonoda, M.; De Schryver, F. C.; Tobe, Y.; De Feyter, S. *J. Am. Chem. Soc.* **2006**, *128*, 3502−3503.
(50) Youngs, W. J.; Djebli, A.; Tessier, C. A. *Organometallics* **1991**, *10*, 2089−2090.
(51) Malaba, D.; Djebli, A.; Chen, L.; Zarate, E. A.; Tessier, C. A.; Youngs, W. J. *Organometallics* **1993**, *12*, 1266−1276.
(52) Zimmermann, B.; Baranović, G.; Štefanić, Z.; Rožman, M. *J. Mol. Struct.* **2006**, *794*, 115−124.
(53) Nishinaga, T.; Miyata, Y.; Nodera, N.; Komatsu, K. *Tetrahedron* **2004**, *60*, 3375−3382.
(54) Hisaki, I.; Eda, T.; Sonoda, M.; Tobe, Y. *Chem. Lett.* **2004**, *33*, 620−621.
(55) Olson, L. P. *J. Mol. Struct. (Theochem)* **2004**, *680*, 65−71.
(56) Boydston, A. J.; Haley, M. M.; Williams, R. V.; Armantrout, J. R. *J. Org. Chem.* **2002**, *67*, 8812−8819.
(57) Jusélius, J.; Sundholm, D. *Phys. Chem. Chem. Phys.* **2001**, *3*, 2433−2437.
(58) Alkorta, I.; Rozas, I.; Elguero, J. *Tetrahedron* **2001**, *57*, 6043−6049.
(59) Tobe, Y.; Fujii, T.; Matsumoto, H.; Tsumuraya, K.; Noguchi, D.; Nakagawa, N.; Sonoda, M.; Naemura, K.; Achiba, Y.; Wakabayashi, T. *J. Am. Chem. Soc.* **2000**, *122*, 1762−1775.
(60) Matzger, A. J.; Vollhardt, K. P. C. *Tetrahedron Lett.* **1998**, *39*, 6791−6794.
(61) Baxter, P. N. W.; Dali-Youcef, R. *J. Org. Chem.* **2005**, *70*, 4935−4953.
(62) Ott, S.; Faust, R. *Synlett* **2004**, 1509−1512.

(63) Ott, S.; Faust, R. *Chem. Commun.* **2004**, 388−389.
(64) García-Frutos, E. M.; Fernández.Lázaro, F.; Maya, E. M.; Vázquez, P.; Torres, T. *J. Org. Chem.* **2000**, *65*, 6841−6846.
(65) Flitsch, W.; Peeters, H. *Chem. Ber.* **1973**, *106*, 1731−1735.
(66) van Roosmalen, J. H.; Jones, E.; Kevelam, H. J. *Tetrahedron Lett.* **1972**, *13*, 1865−1868.
(67) Paudler, W. W.; Stephan, E. A. *J. Am. Chem. Soc.* **1970**, *92*, 4468−4470.
(68) Farquhar, D.; Leaver, D. *Chem. Commun.* **1969**, 24−25.
(69) Baxter, P. N. W. *J. Org. Chem.* **2004**, *69*, 1813−1821.
(70) Baxter, P. N. W. *Chem.—Eur. J.* **2003**, *9*, 2531−2541.
(71) Al Ouahabi, A. Ph.D. Thesis, Institut Charles Sadron, Université de Strasbourg, 2009.
(72) *Top. Curr. Chem.* **2010**, *293*, whole volume.
(73) Kitagawa, S.; Kitaura, R.; Noro, S. *Angew. Chem., Int. Ed.* **2004**, *43*, 2334−2375.
(74) Férey, G. *Chem. Mater.* **2001**, *13*, 3084−3098.
(75) Lauer, M. G.; Leslie, J. W.; Mynar, A.; Stamper, S. A.; Martinez, A. D.; Bray, A. J.; Negassi, S.; McDonald, K.; Ferraris, E.; Muzny, A.; McAvoy, S.; Miller, C. P.; Walters, K. A.; Russell, K. C.; Wang, E.; Nuez, B.; Parish, C. *J. Org. Chem.* **2008**, *73*, 474−484.
(76) Spitler, E. L.; McClintock, S. P.; Haley, M. M. *J. Org. Chem.* **2007**, *72*, 6692−6699.
(77) Johnson, C. A. II; Baker, B. A.; Berryman, O. B.; Zakharov, L. N.; O'Connor, M. J.; Haley, M. M. *J. Organomet. Chem.* **2006**, *691*, 413−421.
(78) Spitler, E. L.; Haley, M. M. *Org. Biomol. Chem.* **2008**, *6*, 1569−1576.
(79) Sugiura, H.; Takahira, Y.; Yamaguchi, M. *J. Org. Chem.* **2005**, *70*, 5698−5708.
(80) Tobe, Y.; Nagano, A.; Kawabata, K.; Sonoda, M.; Naemura, K. *Org. Lett.* **2000**, *2*, 3265−3268.
(81) Megyes, T.; Jude, H.; Grósz, T.; Bakó, I.; Radnai, T.; Tárkányi, G.; Pálinkás, G.; Stang, P. J. *J. Am. Chem. Soc.* **2005**, *127*, 10731−10738.
(82) O'Connor, M. J.; Yelle, R. B.; Zakharov, L. N.; Haley, M. M. *J. Org. Chem.* **2008**, *73*, 4424−4432.
(83) Fabrizi de Biani, F.; Corsini, M.; Zanello, P.; Yao, H.; Bluhm, M. E.; Grimes, R. N. *J. Am. Chem. Soc.* **2004**, *126*, 11360−11369.
(84) Mitzel, F.; Boudon, C.; Gisselbrecht, J.-P.; Gross, M.; Diederich, F. *Chem. Commun.* **2002**, 2318−2319.
(85) Steckler, T. T.; Abboud, K. A.; Craps, M.; Rinzler, A. G.; Reynolds, J. R. *Chem. Commun.* **2007**, 4904−4906.
(86) Mühlbacher, D.; Neugebauer, H.; Cravino, A.; Sariciftci, N. S. *Synth. Met.* **2003**, *137*, 1361−1362.
(87) The reason why **1a** exhibited the highest quantum yield within the series investigated is as yet unclear. However, the result was reproducible using different cells, volumetrics, sources of CH_2Cl_2 solvent, and fluorimeters.
(88) Wang, B.; Wang, F.; Jiao, H.; Yang, X.; Yu, C. *Analyst* **2010**, *135*, 1986−1991.
(89) Atilgan, S.; Ozdemir, T.; Akkaya, E. U. *Org. Lett.* **2010**, *12*, 4792−4795.
(90) Shao, N.; Gao, X.; Wang, H.; Yang, R.; Chan, W. *Anal. Chim. Acta* **2009**, *655*, 1−7.
(91) Bae, J.-S.; Gwon, S.-Y.; Son, Y.-A.; Kim, S.-H. *Dyes Pigm.* **2009**, *83*, 324−327.
(92) Zhan, X.-Q.; Qian, Z.-H.; Zheng, H.; Su, B.-Y.; Lan, Z.; Xu, J.-G. *Chem. Commun* **2008**, 1859−1861.
(93) Nolan, E. M.; Lippard, S. J. *J. Am. Chem. Soc.* **2007**, *129*, 5910−5918.
(94) Changes in the luminescence spectra were also observed to occur over 24−48 h from metal−ligand mixing, which evidenced the slow kinetic formation of the coordination species responsible for the excited state luminescence.
(95) The [14]annulenes **1a−d** were in fact unstable to protonation, undergoing 9−36% loss in absorbance of the λ_{max} upon standing for 14 days in the absence of light at ambient temperature. As protonation kinetics are normally very fast, this observation is consistent with the existence of a parallel proton-induced slow chemical reaction or degradation process, suggesting that the aging of protonated samples has to be considered during the interpretation of spectroscopic protonation studies with these and related systems.
(96) Palacios, M. A.; Wang, Z.; Montes, V. A.; Zyryanov, G. V.; Anzenbacher, P. Jr. *J. Am. Chem. Soc.* **2008**, *130*, 10307−10314.
(97) Sateesh, B.; Soujanya, Y.; Narahari Sastry, G. *J. Chem. Sci.* **2007**, *119*, 509−515.
(98) Wang, Z.; Wu, S. *Chem. Pap.* **2007**, *61*, 313−320.
(99) *Spartan 08*; Wavefunction, Inc.: Irvine, CA. Except for molecular mechanics and semiempirical models, the calculation methods used in *Spartan* have been documented in Shao, Y., et al. *Phys. Chem. Chem. Phys.* **2006**, *8*, 3172−3191.
(100) Becke, A. D. *J. Chem. Phys.* **1993**, *98*, 5648−5652.
(101) Lee., C.; Yang, W.; Parr, R. G. *Phys. Rev. B* **1988**, *37*, 785−789.
(102) Comparison of the calculated geometries with the crystal structures of **1b** and **1c** showed the bond lengths to lie within ±0.02 Å and the calculated inner aryl-ethynyl bond angles to be greater by 0.2−0.8°, confirming that the shape of strained bonds is well reproduced.
(103) Tachibana, H.; Yamanaka, Y.; Sakai, H.; Abe, M.; Matsumoto, M. *Macromolecules* **1999**, *32*, 8306−8309, and references therein.
(104) Zhou, N.; Merschrod, E. F.; Zhao, Y. *J. Am. Chem. Soc.* **2005**, *127*, 14154−14155.
(105) Kijima, M.; Tanimoto, H.; Shirakawa, H. *Synth. Met.* **2001**, *119*, 353−354.
(106) Tagami, K.; Tsukada, M.; Wada, Y.; Iwasaki, T.; Nishide, H. *J. Chem. Phys.* **2003**, *119*, 7491−7497.
(107) Kawakami, T.; Kitagawa, Y.; Matsuoka, F.; Yamashita, Y.; Isobe, H.; Nagao, H.; Yamaguchi, K. *Int. J. Quantum Chem.* **2001**, *85*, 619−635.